Southern Plains Transportation Center
CYCLE 1

FINAL REPORT

2023–2024

USDOT BIL Regional UTC
Region 6

Rapid Assessment of Network-Level Pavement Conditions using Novel Tools

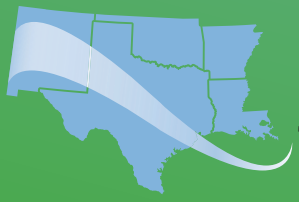

SOUTHERN PLAINS
TRANSPORTATION CENTER

Disclaimer

The contents of this report reflect the views of the authors, who are responsible for the facts and accuracy of the information presented herein. This document is disseminated under the sponsorship of the Department of Transportation University Transportation Centers Program, in the interest of information exchange. The U.S. Government assumes no liability for the contents or use thereof.

Technical Report Documentation Page

1. Report No. CY1-OU-OSU-TTI-06	**2. Government Accession No.**	**3. Recipient's Catalog No.**
4. Title and Subtitle Rapid Assessment of Network-Level Pavement Conditions Using Novel Tools		**5. Report Date** January 15, 2025
		6. Performing Organization Code
7. Author(s) Dr. Sagar Ghos, Dr. Syed Ashik Ali, Kenneth Hobson, Dr. Musharraf Zaman; University of Oklahoma Dr. Joshua Qiang Li; Oklahoma State University		**8. Performing Organization Report No.** CY1-OU-OSU-TTI-06
9. Performing Organization Name and Address School of Civil Engineering and Environmental Science, University of Oklahoma, Norman, Oklahoma School of Civil and Environmental Engineering, Oklahoma State University, Stillwater, Oklahoma		**10. Work Unit No. (TRAIS)**
		11. Contract or Grant No. 69A3552348306
12. Sponsoring Agency Name and Address Southern Plains Transportation Center 202 West Boyd St., Room 213B The University of Oklahoma Norman, OK 73019		**13. Type of Report and Period Covered** Final Report (October 2023 – January 2025)
		14. Sponsoring Agency Code

15. Supplementary Notes
Conducted in cooperation with the U.S. Department of Transportation as a part of University Transportation Center (UTC) program.

16. Abstract
Efficient network-level pavement condition assessment is essential for optimizing maintenance and rehabilitation strategies. Traditional methods, such as visual inspections and manual distress surveys, are often subjective, time-consuming, and inefficient for large-scale pavement management. The focus of this collaborative project was to evaluate tools for rapidly and cost-effectively assessing network-level pavement conditions for Oklahoma. As part of ODOT's engagement in a pooled fund study (TPF-5 (385)), pavement conditions data from I-35 and I-40 in Oklahoma were collected recently using a Traffic Speed Deflectometer (TSD). This study focused on analyzing the TSD data for network-level assessment or rating of the associated pavement. A complementary objective of this study was to collect data from the same pavements using in-house technologies, namely Pave3D 8K available at OSU and an air-coupled Ground Penetrating Radar (GPR) and Fast Falling weight Deflectometer (FFWD) and compare with TSD data. TSD enabled continuous deflection measurements under moving loads, providing a rapid and comprehensive assessment of pavement structural capacity. A total of six pavement sections were selected on the I-35 and I-40 road network in Oklahoma based on the initial TSD rating. These sections were further tested using FFWD, GPR Pave 3D 8K and field investigations. The data from different technologies were used for performing regression analysis using advanced machine learning models. Finally, pavement condition rating parameters and thresholds were proposed for categorizing the pavement sections into good, fair and poor sections. Findings from this research will contribute to the development of a more efficient, data-driven framework for large-scale pavement condition assessment.

17. Key Words Pavement Management System, Pavement Condition Survey, Traffic Speed Deflection Device, Fast Falling Weight Deflectometer, Air-Coupled Ground Penetrating Radar, Pavement Condition Rating	**18. Distribution Statement** No restrictions. This publication is available at www.sptc.org and from the NTIS.

19. Security Classification (of this report) Unclassified	**20. Security Classification (of this page)** Unclassified	**21. No. of Pages** 79 pages	**22. Price** N/A

Form DOT F 1700.7 (8-72) Reproduction of completed page authorized

RAPID ASSESSMENT OF NETWORK-LEVEL PAVEMENT CONDITIONS USING NOVEL TOOLS

FINAL REPORT
SPTC Project Number: CY1-OU-OSU-TTI-06

Submitted by
Dr. Sagar Ghos
Dr. Syed Ashik Ali
Kenneth Hobson
Dr. Musharraf Zaman
School of Civil Engineering and Environmental Science
University of Oklahoma, Norman, Oklahoma

Dr. Joshua Qiang Li
School of Civil and Environmental Engineering
Oklahoma State University, Stillwater, Oklahoma

Prepared for
Southern Plains Transportation Center
The University of Oklahoma
Norman, OK

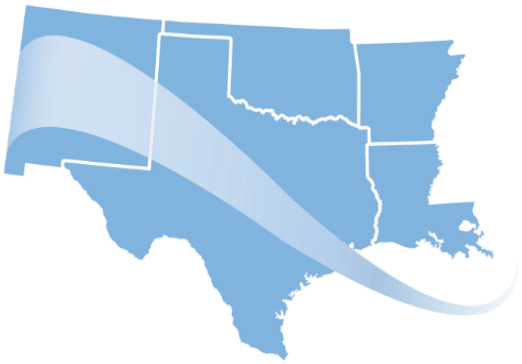

SOUTHERN PLAINS
TRANSPORTATION CENTER

January 2025

Acknowledgments

The authors greatly appreciate the funding provided by the Southern Plains Transportation Center (SPTC) to conduct this research. Also, the support from the Oklahoma Department of Transportation (ODOT) and ODOT District 4 is acknowledged and appreciated. Special thanks to the research team members at Oklahoma State University (OSU), Texas A&M Transportation Institute (TTI) and University of Oklahoma (OU) for their assistance in completing this research. The authors thank the ARRB for their help with TSD data during this study.

Table of Contents

List of Tables

List of Figures

List of Abbreviations and Acronyms

DOT	Department of Transportation
FHWA	Federal Highway Administration
FFWD	Fast Falling Weight Deflectometer
FWD	Falling Weight Deflectometer
GPR	Ground Penetration Radar
PMS	Pavement Management System
TSD	Traffic Speed Deflectometer

Executive Summary

Efficient network-level pavement condition assessment is essential for optimizing maintenance and rehabilitation strategies. Traditional methods, such as visual inspections and manual distress surveys, are often subjective, time-consuming, and inefficient for large-scale pavement management. This study was aimed at the integration of advanced novel tools, namely—Traffic Speed Deflectometer (TSD), Fast Falling Weight Deflectometer (FFWD), Ground Penetrating Radar (GPR), and Pave 3D 8K to assess the pavement condition at network-level. TSD enabled continuous deflection measurements under moving loads, providing a rapid and comprehensive assessment of pavement structural capacity. A total of six pavement sections were selected on the I-35 and I-40 road network in Oklahoma based on the initial TSD rating. These sections were further tested using FFWD tests for complementing TSD in identifying weak sections. GPR aided in subsurface characterization, detecting variations in layer thickness and underlying defects that may compromise pavement integrity. Meanwhile, Pave 3D 8K delivered high-resolution 3D imaging of the pavement surface allowing for distress identification. The data from TSD, FWD and Pave 3D 8K were used for performing regression analysis using advanced machine learning models. Finally, pavement condition rating parameters and thresholds were proposed for categorizing the pavement sections into good, fair and poor sections. The following conclusions and recommendations were drawn from this study:

- TSD provided continuous, high-speed deflection data, enabling network-level structural evaluations without disrupting traffic. TSD deflection basin parameters, namely SCI300, BCI and D1500 with threshold limits from current literature were used for categorizing pavement conditions at network-level. Care should be taken in analyzing the TSD data as it requires significant time and experience. As TSD produces massive amounts of data, care should be taken in cleaning the data before analysis.
- From TSD data analysis, slightly different pavement rankings were observed based on different TSD basin parameters. Based on SCI300 indices, it was observed that most of the I-35 sections were categorized as good conditioned. However, many of the I-40 EB and I-40 WB sections fell under fair to poor categories based on SCI300. It was observed that almost all of I-35 SB and I-40 EB have BCI values less than 76.02 μm, representing good conditions of the pavements. Some sections of I-40 WB were found to exhibit fair conditions from BCI index. Based on D1500, it was observed that most of the I-35 SB, I-40 EB and I-40 WB sections fell under good to fair conditions, indicating strong subgrade layers.
- Pavement surface conditions of the experimental sites identified using TSD analysis were assessed using the Pave3D 8K. The pavement categorization of I-35 experimental sites using rut depths was found to be same as TSD categorization. However, the I-40 experimental sites showed slightly different categorization between TSD and rut depths from Pave3D 8K. For both I-35 and I-40 sites, the MPD results did not match the TSD results. The %CWP and %CWNP from Pave3D 8K were in agreement with the TSD results based on I-35 sites. However, The %CWP and %CWNP results show that the pavement conditions across all I-40 experimental sites are nearly identical, making it challenging to differentiate between them. Therefore, an integrated categorization that considers both structural and functional aspects is essential for the effective management of pavement infrastructure systems.
- Field coring was found to provide insight into pavement categorization using TSD. The I-35 experimental site (Section 2) was found to have a composite structure (concrete over asphalt) and was ranked as good conditioned. Whereas the other two experimental sites consisted of only asphalt materials and were ranked as good and fair conditioned. Also,

the pavement categorization using rut depths from Face Dipstick matched with the ranking obtained from the TSD analysis.

- The FFWD results indicated that the pavement rankings obtained from W1 deflection and E1 modulus are similar to TSD classifications for I-35 experimental sites. The I-40 good experimental site was ranked as good from FFWD W1 deflection and E1 modulus. However, the ranking was the poor- and fair-conditioned experimental sites did not match with TSD ranking.
- The GPR images were found to provide information related to layer thicknesses and subsurface anomalies with potential issues that may not manifest as surface damage. For both I-35 and I-40 experimental sites, the ranking from TSD analysis was found to be in agreement with GPR analysis.
- An attempt was made to determine the correlations between different network-level parameters obtained from the TSD data and in-house technologies using advanced machine learning models. The results suggest that strong correlations between FFWD W1 and E1 with TSD basin parameters allow them to be used interchangeably for assessing pavement structural conditions and ranking at the network-level. It was observed that the %CWP and %CNWP from Pave3D 8K showed moderate fit with SCI300, BCI and AUPP, whereas the RD and MPD did not show any meaningful correlations with TSD basin parameters.
- Based on the collected data and regression analyses, the thresholds for TSD, FFWD and Pave3D 8K parameters were set in such a way that at least 75th percentile data of a particular section fell under that category. The thresholds can be used for classifying the pavement network into good, fair and poor categories for prioritizing pavement maintenance works.

This study highlighted the potential of these advanced technologies in improving cost-effectiveness and resilience in pavement maintenance and rehabilitation, ensuring long-term performance and safety of roadway infrastructure. Findings from this research are expected to contribute to the development of a more efficient, data-driven framework for large-scale pavement condition assessment.

Chapter 1. Introduction

Pavement network is a critical component of the U.S. transportation infrastructure, requiring regular condition monitoring to support cost-effective maintenance, extend service life, manage expenses, and improve driver safety (Khazmin et al., 2017). Currently, 68% of roadway pavements in the U.S. are in poor condition (Peraka & Bilgiri 2020). Without timely interventions, pavement performance can deteriorate significantly, resulting in exponentially higher maintenance and rehabilitation costs. This challenge is becoming increasingly difficult for many states Departments of Transportation (DOTs), specifically for DOTs in Region VI. Therefore, a reliable assessment of pavement conditions with limited resources is essential for making data-driven decisions regarding maintenance, safety, and pavement design.

Transportation agencies collect pavement condition data and populate their Pavement Management System (PMS) to optimize resources for pavement maintenance and rehabilitation. Typically, PMS relies on condition indices or scores to assess roadway pavements at the network-level, though these indices vary across state agencies. Pavement condition data encompasses both structural attributes (e.g., structural number, layer modulus, drainage) and surface attributes (e.g., roughness, rutting, cracking, patching), along with other factors, such as safety, traffic, and accidents to determine overall pavement condition or rating. While structural condition and capacity data are traditionally used at the project level, some agencies are beginning to recognize the value of incorporating these indicators at the network level (Flintsch, & McGhee 2009).

Several tools and technologies are currently available for evaluating pavement structural conditions, including the Falling Weight Deflectometer (FWD), Ground Penetrating Radar (GPR), profilometers, Ultrasonic Pulse Velocity (UPV) devices, Light Detection and Ranging (LiDAR), and Traffic Speed Deflection (TSD) devices. While FWD testing is widely used for assessing pavement structural conditions, it poses safety risks to both testing personnel and the traveling public due to lane closures and other disruptions. In recent years, traffic-speed data collection methods for pavement condition assessment have gained traction, primarily because they do not interfere with traffic flow or require lane closures. TSD is one such technology which can provide data to estimate pavement conditions.

Recent developments have spotlighted the TSD as a valuable technology for measuring surface deflections at short intervals as well as capturing data on roughness, texture, and rutting at traffic speed. As a result, it is gaining popularity among transportation agencies for network-level pavement condition assessment and management. While TSD offers significant benefits in evaluating both surface and structural conditions, challenges remain in using the data to accurately evaluate pavement conditions at network-level. The evaluation of pavement conditions or their rating typically depends on deflection basin parameters, namely deflections, slope deflection indices, structural considerations, and remaining service life. In this context, the potential advantages of deriving network-level pavement condition ratings from TSD data could be greatly enhanced through the implementation of other novel technologies conceived by the collaborative consortium driving this project. It is noted that the scarcity of TSD availability and the expenditure associated with data collection necessitates the pursuit of innovative in-house technologies, which will not only elevate efficiency but also yield cost reductions. The current study focuses on developing a pavement rating system by combining TSD with in-house technologies of partnered institutions.

This collaborative project unites two leading Oklahoma universities – the University of Oklahoma (OU), Oklahoma State University (OSU) and Texas Transportation Institute (TTI) - to

rapidly and cost-effectively assess network-level pavement conditions using novel tools. As part of ODOT's engagement in a pooled fund study (TPF-5 (385)), pavement conditions data from I-35 and I-40 in Oklahoma were collected recently using a TSD. This study focuses on analyzing the collected TSD data for network-level assessment or rating of the associated pavement. A complementary objective was to collect data from the same pavements using in-house technologies, namely Pave3D 8K available at OSU and an air-coupled Ground Penetrating Radar (GPR) and Fast Falling weight Deflectometer (FFWD) available at TTI – a member of the SPTC consortium and compare with TSD data. In addition, this study focuses on investigating the correlation among TSD deflection basin parameters, FFWD structural capacity parameters, and Pave3D 8K parameters using advanced machine learning models.

Chapter 2. Literature Review

2.1 Background

Pavement conditions are typically categorized into functional (level of serviceability) and structural (traffic-carrying capacity and resistance to environmental factors throughout its service life) levels. Both destructive and non-destructive tests are commonly used to evaluate the overall condition of existing pavements. Destructive tests, such as coring, laboratory performance tests, and in-situ tests, are employed by transportation agencies for project-level pavement condition assessments. In contrast, non-destructive tests, including Falling Weight Deflectometer (FWD), Fast Falling Weight Deflectometer (FFWD), Ground Penetrating Radar (GPR), and Pave3D 8K, are used to assess the structural and functional conditions of pavements. Data obtained from these and other tests support pavement management systems (PMS) and help transportation agencies prioritize maintenance, rehabilitation, and reconstruction projects. Some of these measurements can be conducted at traffic speed (e.g., GPR and Pave3D 8K), while others require traffic control measures (e.g., FWD, FFWD, Dynamic Cone Penetrometer (DCP), and seismic cone testing). Traffic control increases cost, time, and safety risks. As a result, pavement condition assessment using traffic-speed data is gaining national momentum. In this context, the Traffic Speed Deflectometer (TSD) is increasingly attracting the attention of state DOTs, including the DOTs in Region 6. TSD enables the assessment of both structural and functional pavement conditions without the need for traffic control, offering a more efficient and safer alternative.

2.2 Pavement Condition Evaluation using Falling Weight Deflectometer (FWD)

Since the 1980s, the Falling Weight Deflectometer (FWD) has been one of the most widely used devices for pavement condition assessment in the U.S. In this test, a deflection basin is measured under an impact load using geophone sensors. The size of the loading plate and the magnitude of the impact load depend on the material being tested (e.g., asphalt, stabilized subgrade, compacted subgrade).

Typically, an impact load is applied to a circular plate 12 inches (300 mm) in diameter, placed on the pavement surface. The load is normalized to 9 kips (40 kN), equivalent to half an Equivalent Single Axle Load (ESAL). Transportation agencies generally rely on the deflection at the center of the plate to assess the overall structural capacity of the pavement. The deflection measured directly beneath the center of the load (D0) is typically considered the maximum deflection. Additionally, FWD collects deflections at distances of 12 inches (300 mm), 24 inches (600 mm), 36 inches (900 mm), 48 inches (1200 mm), 60 inches (1500 mm), and 72 inches (1800 mm) from the plate center. These deflections, along with pavement thickness data, are used to determine the modulus of various pavement layers, including the subgrade soil, as an indicator of stiffness. Figure 1 illustrates the stress distribution and measured deflection bowl beneath the FWD.

Recently, modifications have been made to the FWD to accelerate pavement testing and enable quicker decision-making. The Fast Falling Weight Deflectometer (FFWD) is the next-generation FWD, capable of testing pavements at least five times faster than traditional FWD testing (Dynatest 2025). However, FFWD still requires lane closures for operation.

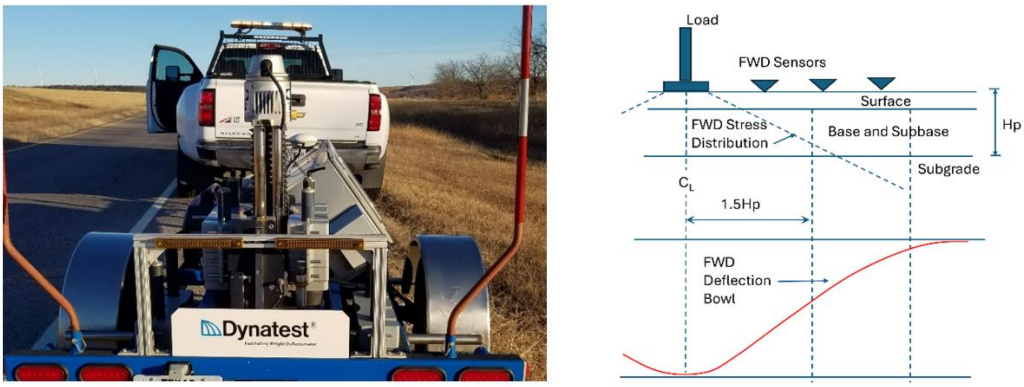

(a) (b)

Figure 1 (a) A photographic view of Falling Weight Deflectometer, and (b) measurement approach

2.3 Pavement Condition Evaluation using Traffic Speed Deflectometer (TSD)

TSD is an instrumented truck that applies a rear axle load ranging from 13 to 28 kips onto the pavement surface. It is typically equipped with seven Doppler laser sensors positioned at 0, 8 inches (200 mm), 12 inches (300 mm), 24 inches (400 mm), 36 inches (600 mm), 48 inches (800 mm), 60 inches (1000 mm), and 72 inches (1200 mm) in front of the loaded axle (i.e., in the direction of traffic). Additionally, a single laser sensor is located outside the deflection bowl, serving as the reference sensor (Katicha et al., 2017).

TSD can be operated at various speeds; however, a speed of 60 MPH with a data collection rate of 1 kHz is commonly used (Katicha et al., 2017). The device determines the deflection slope by measuring the vertical pavement deflection velocity and the horizontal velocity of the vehicle at each laser sensor location. Using these data, a deflection basin is generated, representing the profile of the deflected pavement. Pavement deflection is then obtained by integrating the deflection slope. Figure 2 provides a pictorial representation of this approach.

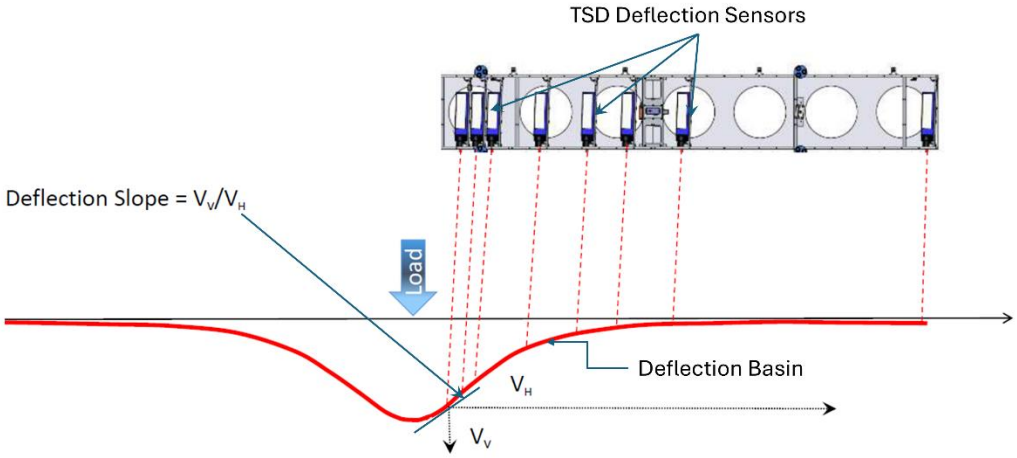

Figure 2 Deflection slope from Traffic Speed Deflection Device

2.4 Comparison of TSD and FWD Measurements

The primary differences between FWD and TSD measurements lie in the nature of loading and the type of measuring sensors. The FWD applies an impact load, while the TSD uses a moving half-axle load. Additionally, FWD relies on geophones for deflection measurement, whereas TSD uses laser sensors.

Another key distinction is the testing procedure. In FWD testing, multiple drops are used to verify repeatability, whereas TSD data are collected continuously at close intervals as the instrumented truck moves at traffic speed. Some accuracy may be lost in TSD due to the averaging process and the method used to define pavement deflection—issues that are not present in FWD testing. Furthermore, during TSD testing, stress and strain tensors rotate, whereas in FWD testing, they remain constant. Other factors influencing TSD data include damping, tire pressure, and truck dynamics (Rada & Nazarian, 2011). Therefore, careful evaluation of TSD data and the correlation methods used in assessing pavement condition indices is essential.

2.5 Deflection Basin Parameters

Over time, numerous studies have proposed deflection basin-related indices or deflection bowl parameters to analyze deflection data from deflectometers. These parameters primarily focus on the maximum deflection under the center of the load and variations in deflection among sensors as indicators of the stiffness of different pavement layers, including the subgrade, and the pavement's remaining life. A summary of the most influential parameters, formulas, and structural indicators derived from measured deflections is provided in Table 1.

Table 1 Deflection Bowl Parameters (Schooner & Horak 2012)

Parameter	Formula	Structural indicator
1. Maximum Deflection	D_0 as measured	An indication of all structural layers with about 70% contribution by the subgrade
2. Radius of Curvature (RoC)	$\mathrm{RoC} = L^2/(2D_0[(\frac{D_0}{D_{200}}) - 1]$ where, L=127 mm in the Dehlen curvature meter and 200 mm for the FWD	An indicator of the structural condition of the surface and base layers
3. Base Layer Index (BLI) also known as Surface Curvature Index (SCI)	SCI = BLI = $D_0 - D_{300}$	An indicator of structural condition of primarily the base layer
4. Middle Layer Index (MLI) also known as Base Damage Index (BDI)	BDI = MLI = $D_{300} - D_{600}$	An indicator of structural condition of the subbase and probably selected layers
5. Lower Layer Index (LLI) also known as Base Curvature Index (BCI)	BCI = LLI = $D_{600} - D_{900}$	An indicator of condition of the lower structural layers like a selected layer and the subgrade layer
6. Spreadability, S	$S = \frac{\{[\frac{D_0 + D_{300} + D_{600} + D_{900}}{5}] 100\}}{D_0}$	Supposed to reflect the structural response of the whole pavement structure, but with weak correlations
7. Area, A	$A = \frac{6[D_0 + 2D_{300} + 2D_{600} + D_{900}]}{D_0}$	Supposed to reflect the structural response of the whole pavement structure, but with weak correlations
8. Shape factors	$F1 = (D_0 - D_{600})/D_{300}$ $F2 = (D_{300} - D_{900})/D_{600}$	The F2 shape factor seems to give better correlations with subgrade moduli while F1 seems to give weak correlations
9. Slope of Deflection	$SD = \tan^{-1}(D_0 - D_{600})/600$	Weak correlations observed
10. Additional shape factor	$F3 = (D_{600} - D_{1200})/D_{900}$	Condition of lower layer or depth to a stiff layer
11. Area under pavement profile	$AUPP = \frac{(5D_0 - 2D_{300} - 2D_{600} - D_{900}}{2}$	Characteristics of the pavement upper layers
12. Additional areas	$A2 = \frac{6(D_{300} + 2D_{450} + D_{600})}{D_0}$ $A3 = \frac{6(D_{600} + 2D_{900} + D_{1200})}{D_0}$	Condition of middle layer Condition of lower layers

Parameter	Formula	Structural indicator
13. Area indices	$\mathrm{AI1} = (\mathrm{D}_0 + \mathrm{D}_{300})/2\mathrm{D}_0$ $\mathrm{AI2} = (\mathrm{D}_{300} + \mathrm{D}_{600})/2\mathrm{D}_0$ $\mathrm{AI3} = (\mathrm{D}_{600} + \mathrm{D}_{900})/2\mathrm{D}_0$ $\mathrm{AI4} = (\mathrm{D}_{900} + \mathrm{D}_{1200})/2\mathrm{D}_0$	Condition of upper layer Condition of middle layer Condition of middle layer Condition of lower layer

The aforementioned indices are commonly used to assess pavement condition. The Virginia Department of Transportation (VDOT) has selected the Deflection Slope Index (DSI) and the Surface Curvature Index at 300 mm (SCI300) for pavement condition evaluation using TSD. The DSI is defined as the difference between deflections at 100 mm and 300 mm (D100 - D300) (Katicha et al., 2017).

Additionally, several deflection parameters, as presented in Equations (1) through (5), were proposed by Rada et al. (2016) and are currently used by the Federal Highway Administration (FHWA) for pavement condition assessment.

$$R1r = \frac{r^2}{2Do\left(1-\frac{Dr}{Do}\right)} \quad (1)$$

$$R2r = \frac{r^2}{2Do\left(\frac{Do}{Dr}-1\right)} \quad (2)$$

$$SCI = D_0 - D_r \quad (3)$$

$$DSI_{s\text{-}r} = D_s - D_r \quad (4)$$

$$SD_r = \frac{\tan^{-1}(D_0 - D_r)}{r} \quad (5)$$

where,

r, s = distance from applied load in inches (s>r);
D_x = deflection at distance x from the load; and
D = differential operator.

2.6 Pavement Condition Indices for Assessment of Network-Level Pavement Conditions

In recent years, several studies have focused on developing Pavement Condition or Quality Indices to categorize pavement sections into good, fair, and poor conditions (Zhang et al., 2003; Bryce et al., 2011; Horak et al., 2015; Shrestha, 2017). For example, Zhang et al. (2003) developed a methodology for structural characterization of pavement conditions. Internal studies at the Texas Department of Transportation (TxDOT) indicated that the Structural Strength Index (SSI) was not sensitive enough to differentiate between pavements requiring structural reinforcement and those that did not. The primary objective of Zhang et al. (2003)'s research was to develop a structural index, based on FWD data, that could effectively distinguish between pavements needing additional structural capacity and those for which surface treatments would suffice. Comprehensive guidelines were established for utilizing the Structural Condition Index (SCI) in selecting the most appropriate maintenance and rehabilitation strategies at the network level. A pilot study was also conducted on several pavement rehabilitation projects to validate the effectiveness of the SCI.

Bryce et al. (2011) developed a structural index known as the Modified Structural Index (MSI) for use in network-level pavement evaluation. The MSI is a modified version of the Structural

Condition Index (SCI) and is integrated into the Virginia Department of Transportation's Pavement Management System (PMS). Network-level predictions identified MSI as the most promising index for predicting project-level maintenance and rehabilitation activities. MSI can be used as a network-level screening tool, for deterioration modeling, and in the development of structural performance measures. However, MSI is applicable only to flexible pavements, as it is based on FWD data and is empirical in nature (Bryce et al., 2011).

Horak et al. (2015) developed a benchmark analysis methodology that utilizes the embedded structural response knowledge of the entire deflection bowl, as measured by the FWD, for comparative evaluation of the structural condition of flexible pavement structures. In that study, three deflection basin parameters - Modified Structural Number (SNP), Pavement Number (PN), and Structural Condition Index (SCI) - were calculated from full deflection bowls and used in enhanced benchmark analyses of flexible pavement structures.

Shrestha (2017) conducted a field evaluation of the TSD to classify pavement structural conditions for a small subset of the Pennsylvania secondary road network. In that study, an Overall Pavement Index (OPI) was developed using TSD data to categorize pavements into good, fair, and poor conditions. The OPI was derived from a model that relates pavement surface characteristics to pavement age and Structural Number (SN). The threshold separating pavements with good surface conditions from those with fair conditions was obtained from the Pennsylvania Pavement Management System (PMS). Using the determined OPI values and model equations, Deflection Slope Index (DSI) thresholds were calculated. The OPI thresholds for different pavement conditions were then used to establish corresponding DSI thresholds. This was achieved by identifying the DSI values associated with each OPI threshold category for pavements with a 10-year-old surface (Shrestha, 2017).

To effectively characterize pavement conditions using TSD data, it is essential to establish appropriate thresholds for pavement quality indicators. To this end, existing literature on TSD-related pavement quality indicator thresholds was reviewed and discussed in the following section.

2.7 Threshold Values for Pavement Condition Indices

In recent years, several studies have been conducted to establish thresholds for TSD basin parameters to characterize pavement conditions. For example, the Virginia Tech Transportation Institute proposed using temperature-corrected (70°F) structural indices derived from TSD deflection basins to categorize pavement sections as Good, Fair, or Poor. This method utilized SCI300 and DSI, with results showing similar trends for both indices. Preliminary thresholds distinguishing Good, Fair, and Poor structural conditions were provided in the Virginia Tech Transportation Institute report, based on estimates of the expected remaining fatigue life of the asphalt layer. The recommended thresholds are summarized in Table 2.

The Pennsylvania Department of Transportation (PennDOT) employs DSI to classify pavement quality into Poor, Fair, and Good categories. Table 3 presents the DSI threshold values suggested by PennDOT, which apply specifically to the non-National Highway System (non-NHS). In this study, both SCI300 and DSI are used to characterize pavement conditions. The TxDOT guidelines to assign PMIS treatment levels using SCI, BCI and W7 indices are presented in Table 4.

Table 2 Virginia Tech Transportation Institute TSD Thresholds for Pavement Category

Road Category	AC Layer Thickness (in.)	Annual Traffic, ESAL (million)	Threshold for Fatigue Cracking at Wheel path (%)	Threshold for Poor, Nf, Million ESAL	Threshold for Poor, SCI300 (mil)	Threshold for Poor, DSI (mil)	Threshold for Fair, Nf, million ESAL	Threshold for Fair, SCI300 (mil)	Threshold for Fair, DSI (mil)
Interstate	>9	1.4	10	2.8	3.7	3.0	7.0	2.7	2.2
Primary	6-9	0.2	10	0.4	6.2	5.2	1.0	4.9	4.0
Secondary	3-6	0.07	45	0.14	9.7	7.7	0.35	7.3	5.8

Table 3 PennDOT DSI Thresholds for Pavement Category

Non-NHS: AADT	Pavement Condition	DSI	Non-NHS: AADT	Pavement Condition	DSI
≥ 2000	Good	<0.39	<2000	Good	<5.90
≥ 2000	Fair	0.39-9.78	<2000	Fair	5.90-15.90
≥ 2000	Poor	>9.78	<2000	Poor	>15.90

Table 4 TxDOT DSI Thresholds for Pavement Category

Index Parameters	Thicknes s>5	Thickness ≤5, ≥2.5	Thickness <2.5, ≥1	Thickness <1	Diagnosis
SCI	<4	<6	<12	<16	Very Good Asphalt Layer
SCI	<4	<6	<12	<16	Good Asphalt Layer
SCI	4-6	6-10	12-18	16-24	Fair Asphalt Layer
SCI	6-8	10-15	18-24	24-32	Poor Asphalt Layer
SCI	8-10	15-20	24-30	32-40	Very Poor Asphalt Layer
BCI	>10	>20	>30	>40	Very Good Baset Layer
BCI	<2	<3	<4	<8	Good Base Layer
BCI	2-3	3-5	4-8	8-12	Fair Base Layer
BCI	3-4	5-9	8-12	12-16	Poor Asphalt Layer
BCI	4-5	8-10	12-16	16-20	Very Poor Base Layer
W7	>5	>10	>16	>20	Very Good Subgrade Layer
W7	<1	<1	<1	<1	Good Subgrade Layer
W7	1-1.4	1-1.4	1-1.4	1-1.4	Fair Subgrade Layer
W7	>1.4-1.8	>1.4-1.8	>1.4-1.8	>1.4-1.8	Poor Subgrade Layer
W7	>1.8-2.2	>1.8-2.2	>1.8-2.2	>1.8-2.2	Very Poor Subgrade Layer

Chapter 3. Materials and Methodologies

This chapter outlines the detailed methodology adopted in this study. A high-level overview of the methodology adopted in this study is illustrated in the workflow diagram (Figure 3). For the purpose of this study, pavement condition data from I-35 and I-40 in Oklahoma, recently collected as part of ODOT's engagement in a pooled fund study (TPF-5 (385)) using a TSD, was collected and analyzed. A comprehensive set of pavement condition indicators were determined by analyzing the TSD data. Leveraging these indicators, the I-35 and I-40 pavement sections were divided into three different categories, namely poor, fair, and good. Based on this categorization, experimental sites were selected for an in-depth evaluation. These initially rated sections were then further used for in-depth evaluation using FFWD, GPR and Pave3D 8K. GPR images were calibrated and validated by collecting field cores at selected locations. Structural capacities of these sections were evaluated using FFWD tests at every 10^{th} of a mile. Pavement surface characteristics of these test sites, namely rut depth (RD), mean depth profile (MDP), cracking along wheel path (CWP), and cracking along non-wheel path (CNWP) were evaluated using the Pave3D 8K. Advanced machine learning models including linear regression, gradient boosting regression, decision tree, random forest, KNeighbors regressor, and Huber regression were used to investigate the correlation between TSD deflection basin parameters, FFWD structural performance parameters and Pave3D 8K surface parameters. Finally, a pavement rating limit was developed using TSD, FFWD and Pave3D 8K. The following subsections provide a detailed discussion of these methodologies.

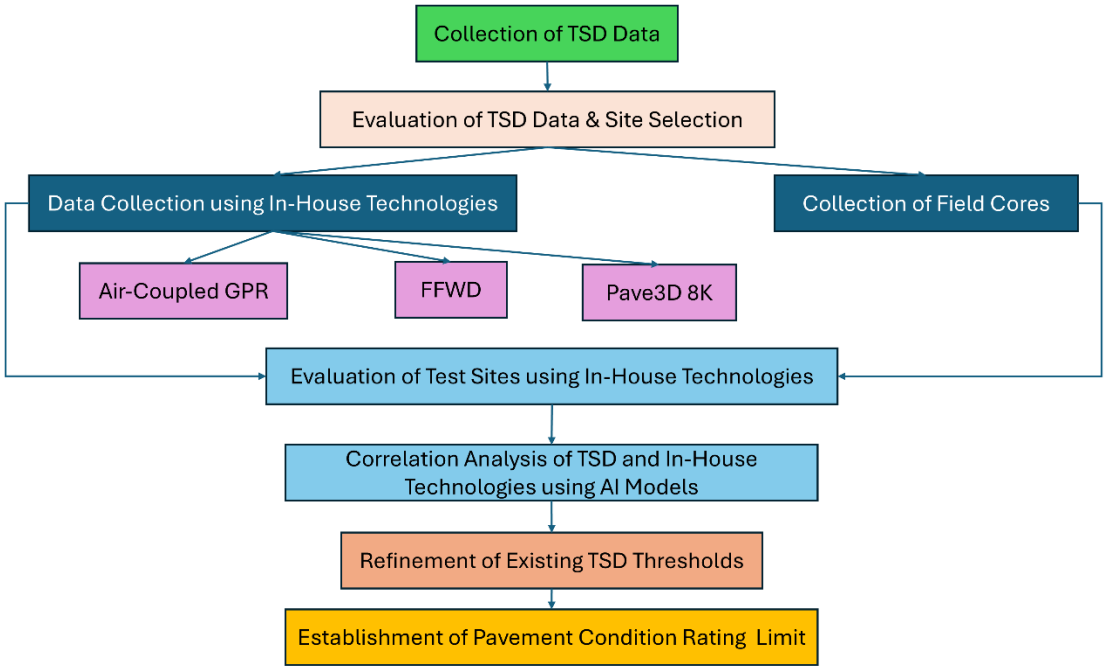

Figure 3 Workflow Diagram

3.1 Collection of TSD Data

With the assistance of Strategic Asset and Performance Management (SAPM) personnel at ODOT, the research team gained access to recently collected TSD data from I-35 and I-40. It was found that the TSD data was collected from three highway segments, namely Interstate-35 Southbound (I-35 SB), Interstate-40 Eastbound (I-40 EB), and Interstate-40 Southbound (I-40

SB). Figure 4 shows the satellite view of the different segments. The I-35 segment begins with Hunnewell (36.399916, -97.327006) and ends at I-35/I40 junction (35.46651, -97.46871). The TSD data was collected on the southbound lane of I-35. The I-40 EB travels from Texola (35.2267, -100.0013) towards I-35/I-40 junctions (35.4500, -97.4331). The I-40 WB runs from I-35/I-40 junction (35.46561, -97.469490) towards Texola (35.2271, -100.00125).

Figure 4 Google Earth View of Test Sites

The ODOT Pavement Management personnel provided the OU team access to the Hawkeye website which is the online storage of TSD data. Figure 4 shows a snippet of the Hawkeye website. After evaluating the available data on the Hawkeye website, it was determined that access to raw TSD data was required to determine different pavement condition indicators. ODOT helped the OU team to get access to the raw data from Australian Road Research Board (ARRB). Figure 5 shows a snippet of the raw data spreadsheet collected from ARRB.

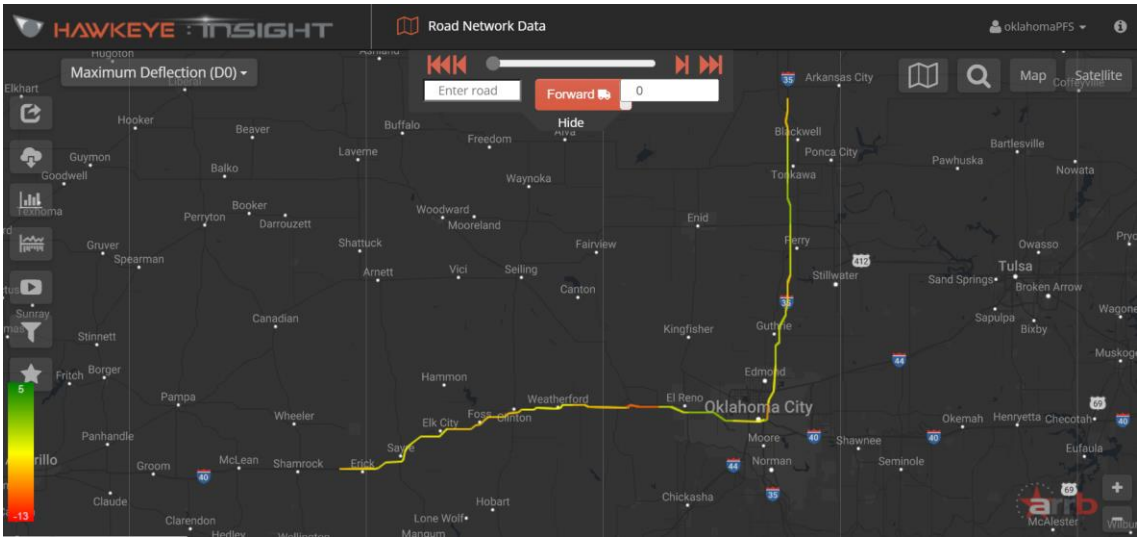

Figure 5 A snippet of the Hawkeye website

Data:
Chainage [m]| Driving Speed [m/s]| Driving Accl [m/s²]| GyroYaw [rad/s]| GyroRoll [rad/s]| GyroPitch [rad/s]| AcclLoad [m/s²]| AcclVerti 1.9[m/s²]| AcclTrans [m/s²]| AcclHoris [m/s²]| Strain Gauge Left [kg]| Strain Gauge Right [kg]| LinPot 2.845[mm]| LinPot 0.825[mm]| Frequency Fan Speed 1[m/s]| Frequency Fan Speed 2[m/s]| Frequency Fan Speed 3[m/s]| Frequency Fan Speed 4[m/s]| Temp Road [°C]| PWM Temperature 1[°C]| Temp Air [°C]| Temp Inside 8.4[°C]| Temp Inside 3.4[°C]| Temp BeamHigh 3.4[°C]| Temp BeamLow 3.4[°C]| Temp BeamHigh 2.2[°C]| Temp BeamLow 2.2[°C]| Temp BeamHigh 0.5[°C]| Temp BeamLow 0.5[°C]| Doppler 3.080[m/s]| Doppler 1.500[m/s]| Doppler 0.900[m/s]| Doppler 0.600[m/s]| Doppler 0.450[m/s]| Doppler 0.300[m/s]| Doppler 0.215[m/s]| Doppler 0.130[m/s]| Doppler -0.200[m/s]| Doppler -0.300[m/s]| Doppler -0.450[m/s]| DeflVel 1.500[mm/s]| DeflVel 0.900[mm/s]| DeflVel 0.600[mm/s]| DeflVel 0.450[mm/s]| DeflVel 0.300[mm/s]| DeflVel 0.215[mm/s]| DeflVel 0.130[mm/s]| DeflVel -0.200[mm/s]| DeflVel -0.300[mm/s]| DeflVel -0.450[mm/s]| Slope 1.500[µm/m]| Slope 0.900[µm/m]| Slope 0.600[µm/m]| Slope 0.450[µm/m]| Slope 0.300[µm/m]| Slope 0.215[µm/m]| Slope 0.130[µm/m]| Slope -0.200[µm/m]| Slope -0.300[µm/m]| Slope -0.450[µm/m]| DoppValidity 3.080| DoppValidity 1.500| DoppValidity 0.900| DoppValidity 0.600| DoppValidity 0.450| DoppValidity 0.300| DoppValidity 0.215| DoppValidity 0.130| DoppValidity -0.200| DoppValidity -0.300| DoppValidity -0.450| SCI200 [µm]| SCI300 [µm]| SCISUB [µm]| D-450[µm]| D-300[µm]| D-200[µm]| D0[µm]| D200[µm]| D300[µm]| D450[µm]| D600[µm]| D900[µm]| D1200[µm]| D1500[µm]| Goodness of fit
0.0000| 30.9773| -0.4301| 0.0015| -0.0030| -0.0033| 0.0718| -0.0516| 0.0789| 0.3758| 3048.6149| 4835.2401| -1.7792| 0.5742| 47.1321| 47.4655| 48.3965| 45.7988| 37.4503| 30.8355| 30.4684| 22.2929| 22.3161| 22.2096| 22.0818| 21.9623| 22.5792| 21.9021| 21.5921| 0.0457| 0.0502| 0.0407| 0.0355| 0.0427| 0.0218| 0.0422| 0.0251| 0.0345| 0.0365| 0.0197| 0.1713| 0.5570| -0.1814| 0.4912| -0.4445| -0.0707| -1.5960| -0.3754| -3.4601| -3.0751| 5.5284| 17.9797| -5.8563| 15.8560| -14.3501| -2.2839| -51.5218| -12.1199| -111.6969| -99.2711| 0.4569| 0.5300| 0.5269| 0.4058|

Figure 6 A snapshot of TSD data collected on the I-35 section

3.2 Analysis of TSD Data and Selection of Experimental Sites

The team conducted a literature review to identify the pavement condition indices and thresholds that could be used to evaluate the pavement conditions at network-level. Drawing on these literature reviews, a comprehensive set of pavement condition indicators encompassing Surface Curvature Index (SCI), Base Curvature Index (BCI), Area Under Pavement Profile (AUPP) and D1500 were employed to analyze the TSD data. Leveraging these indicators, the I-35 and I-40 pavement sections were divided into three different categories, namely poor, fair, and good. Table 5 presents the thresholds of TSD pavement condition indices used in this study. These thresholds were chosen based on existing literature and discussions with the collaborative partners. As can be seen from Table 5, the thresholds for SCI300 were selected from the specification proposed by Virginia Tech Transportation Institute. The pavement categorization thresholds for BCI and D1500 were selected based on TxDOT and TDOT specifications. This categorization facilitated the subsequent selection of experimental sites for an in-depth evaluation, each spanning a length of 10 to 15 kilometers (km). Based on these analysis, three experimental sites to represent three pavement categories, namely poor, fair, and good from I-35 were selected. Similarly, another three experimental sites were selected from I-40.

Table 5 Thresholds of pavement condition indices obtained from TSD

Category	SCI300, µm (Asphalt Layer) Virginia Tech Transportation Institute)	BCI, µm (Base Layer) (TxDOT)	D1500, µm (Subgrade Layer) (TDOT)
Good	<68.58	<76.2	<25.4
Fair	68.58-93.98	76.2-101.6	25.4-55.88
Poor	>93.98	>101.6	>55.88

3.3 Collection and Analysis of Data using Pave3D 8K Data

As mentioned earlier, six testing sites, among which three sites were located on I-35 and three sites on I-40, were selected based on the TSD data. Surface image data and detailed pavement condition and texture data were acquired from these sites using Pave3D 8K. During the field data collection, there was no interruption of traffic on I-35 and I-40 as the field data was collected at traffic speed. The Pave3D 8K system (Figure 7) is a sophisticated system to

conduct full lane data collection on roadways at highway speed up to 60mph with 0.5mm resolution. It can acquire both laser imaging intensity (2D) and range data (3D) from pavement surfaces through two separate sets of sensors. In addition, two 3D high-resolution digital accelerometers are installed on the system. These accelerometers are capable of compensating pavement surface profiles and generating roughness indices. The 0.5mm 3D pavement surface data can be used for the following:

- Comprehensive evaluation of surface distresses, with automatic and interactive detection of cracks and classifying them based on various protocols;
- Safety analysis, including macrotexture in terms of mean profile depth (MPD) and mean texture depth (MTD), hydroplaning prediction, and grooving identification and evaluation;
- Roadway geometry, including horizontal curve, longitudinal grade, and cross slope.

Figure 7 Pave3D 8K system for field data collection

Once the pavement surface data was collected from the field using Pave3D 8K, the next step was to process the raw data using the ADA 3D software to obtain different pavement condition parameters, such as roughness, rutting, crack categorization (including type, severity, and density), and patching. Figure 8 shows the different screenshots of ADA3D software during the processing of raw data, and Figure 9 shows the screenshot for rut depth calculation. Once the computation was completed, the results were exported into .csv formatted files for further analysis.

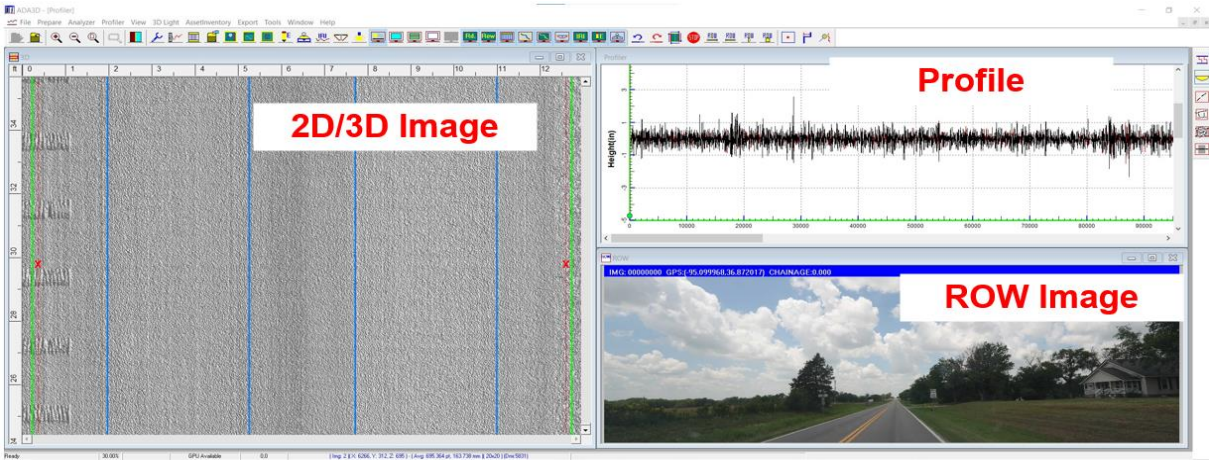

Figure 8 Interface of ADA-3D Software

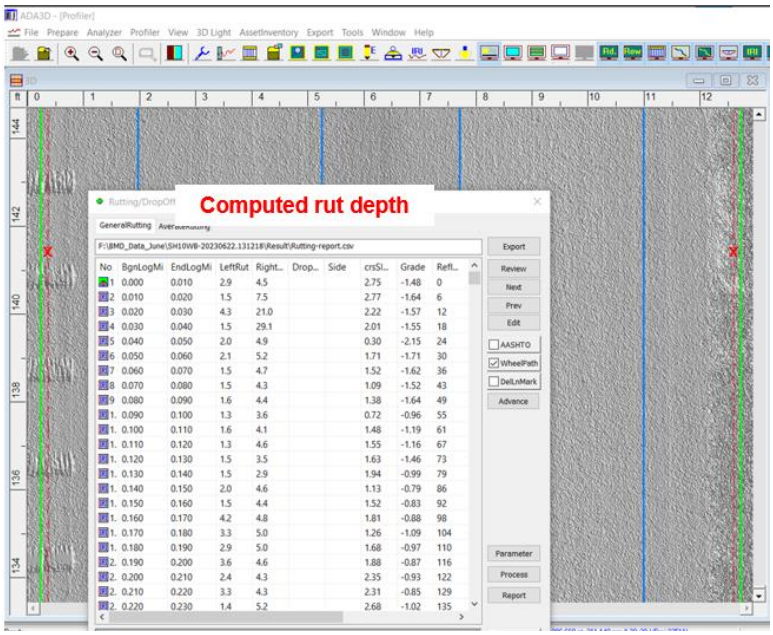

Figure 9 Computation Interface of Rut Depth Using ADA 3D

3.4 Collection of FFWD Test Data

FFWD tests were conducted by Texas Transportation Institute (TTI) at the selected I-35 and I-40 sections using the available facility (Figure 10). The goal was to conduct these tests at the same or close locations as TSD. For the convenience of the test, FFWD data was collected at every 10th of a mile. Measured deflections were analyzed using Modulus 7.0. The analyzed data was used to determine structural conditions and compare with the corresponding TSD results. These comparisons were useful for setting the rating limits. The test was conducted at night to avoid heavy traffic on the interstate highways. Rolling traffic control for FFWD testing was provided by the associated ODOT field districts.

Figure 10 FFWD data collection on I-35 test section

3.5 Collection of GPR Data

A subsurface GPR survey was conducted on the above mentioned I-35 and I-40 sections with the help of TTI on June 24, 2024. A 1 GHz horn antenna system with integrated high-definition video and GPS was used for this purpose. Data was collected at highway speed with no traffic control. The GPR data was processed with the software developed by TTI to compute layer thicknesses and used to identify areas with subsurface defects. Figure 11 shows the photograph of the TTI's GPR equipment.

Figure 11 Photographic View of TTI's Air Coupled GPR

3.6 Collection of Selective Cores from Distressed Locations

Based on the TSD and FFWD test results, cores were extracted selectively from distressed locations of experimental sites. Considering the limitations of this study, cores were collected from only three I-35 experimental sites representing poor, fair and good conditions. For the purpose of comparison, cores were collected from few non-distressed locations. A visual observation of the extracted cores as well as limited laboratory test were used to validate the pavement rating obtained from the TSD data. Traffic control for coring was provided by the associated field districts. In addition to field core collection, roadway profiles in the selected locations were surveyed using Face Dipstick and Straight Edge. Figures 12, 13 and 14 show the Straight Edge measurement, Face Dipstick test and coring operations.

Figure 12 Face Dipstick Measurements on I-35 Test Site

Figure 13 Roadway Profile Measurement using Face Dipstick

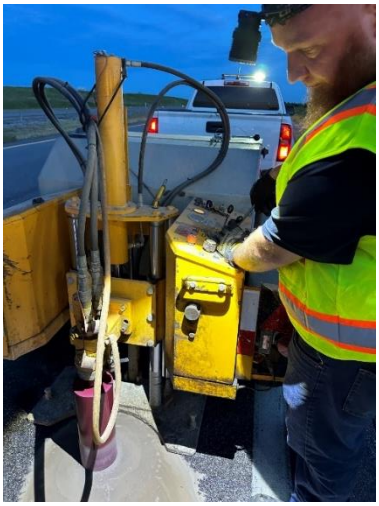

Figure 14 Coring Operations on I-35 Test Site

3.7 Comparison of Different Technologies and Determining Pavement Condition Rating Limits:

The collaborative teams worked together to compare the results from different technologies and established pavement condition thresholds. In this study, the correlation among TSD basin parameters, FFWD structural capacity parameters and Pave3D 8K parameters were studied using advanced machine learning models in order to develop pavement rating limits for both flexible and rigid pavements. For the purpose of this study, a total of 52 machine learning models were initially studied and finally 6 of them were finally selected for studying correlations. Both single and multivariate analyses were performed to evaluate the individual and combined effects of all these variables. Once the correlations were established, a rating limit system was proposed based on TSD, FFWD and Pave3D 8K performance parameters. A brief description of six selected machine learning models is provided below:

3.7.1 Linear Regression:

Linear regression is a fundamental statistical technique used to model and analyze the relationship between a dependent variable and one or more independent variables (Sohil et al. 2022). It helps in predicting the value of the dependent variable based on the values of the

independent variables. Linear regression assumes a linear relationship between the dependent variable (Y) and the independent variables (X). The model can be represented as:

$$\boldsymbol{Y = \beta_0 + \beta_1 X_1 + \beta_2 X_2 + \cdots + \beta_n X_n + \epsilon} \quad (1)$$

Where,

β_0 is the intercept
$\beta_1, \beta_2, \ldots, \beta_n$ are the coefficients for the independent variables
ϵ is the error term

The goal is to find the values of the coefficients (β) that minimize the difference between the observed and predicted values of the dependent variable. This is typically done using the least squares method. The performance of the linear regression model can be evaluated using metrics, such as R-squared, adjusted R-squared, Mean Absolute Error (MAE), Mean Squared Error (MSE), and Root Mean Squared Error (RMSE).

3.7.2 Gradient Boosting Regressor

Gradient Boosting Regressor is a powerful machine learning algorithm used for regression tasks. It is part of the ensemble learning family, where multiple weak models (typically decision trees) are combined to create a strong predictive model. Gradient Boosting Regressor builds an ensemble of weak prediction models, typically decision trees, in a sequential manner to minimize the residual errors. The prediction at step m is updated as,

$$\boldsymbol{F_m(x) = F_{m-1}(x) + \gamma_m h_m(x)} \quad (2)$$

where,

$F_m(x)$ is the updated model at iteration m.
$F_{m-1}(x)$ is the model from the previous iteration.
$h_m(x)$ is the weak learner (typically a decision tree) trained to minimize the residual errors.
γ_m is the learning rate, controlling the contribution of each weak learner.

The model is trained iteratively by reducing the loss function (MSE) using gradient descent, leading to improved predictive performance with each iteration.

3.7.3 Decision Tree Regressor

A Decision Tree Regressor is a non-parametric supervised learning algorithm used for regression tasks. It works by recursively splitting the data into subsets based on feature values, creating a tree-like structure where each internal node represents a decision rule, and each leaf node holds a predicted value. The model selects splits by minimizing a chosen error metric, such as MSE or mean absolute error (MAE). Decision Tree Regressor models a target variable Y as a hierarchical structure of decision rules based on input features X. It recursively partitions the feature space into smaller regions and assigns a constant prediction to each region. The model represents as follows:

$$\hat{\boldsymbol{y}} = \frac{\boldsymbol{1}}{\boldsymbol{N}} \sum_{\boldsymbol{i \in R_j}} \boldsymbol{y_i} \quad (3)$$

where,

$\hat{y}$ is the predicted value at a leaf node
Rj is the region (subset of data) associated with a leaf node
yi are the actual target values in Rj
N is the number of samples in Rj

The splits are chosen by minimizing an impurity function, such as the MSE. The tree grows until a stopping criterion is met, such as a minimum number of samples per leaf or maximum depth. To prevent overfitting, techniques like pruning or setting constraints on depth and leaf size are commonly used.

3.7.4 Random Forest Regressor

A Random Forest Regressor is an ensemble learning method that combines multiple decision trees to improve prediction accuracy and reduce overfitting. It operates by training multiple decision trees on different random subsets of the data and averaging their output for regression tasks. The model can be represented as:

$$\hat{y} = \frac{1}{M}\sum_{m=1}^{M} T_m(x) \quad (4)$$

where,

$\hat{y}$ is the final predicted value
M is the number of decision trees in the forest
$T_m(x)$ is the prediction from the m^{th} decision tree.

Each tree is trained on a bootstrapped sample of the training data, and at each split, a random subset of features is considered to enhance diversity among trees. This randomness helps in reducing variance while maintaining predictive power.

3.7.5 K-Neighbors Regressor

The K-Nearest Neighbors (KNN) Regressor also known as K-Neighbors Regressor is a non-parametric algorithm that predicts the target value of a given input by averaging the target values of its k nearest neighbors in the feature space. It is based on the assumption that similar inputs have similar outputs. The model is represented as:

$$\hat{y} = \frac{1}{k}\sum_{i=1}^{k} y_i \quad (5)$$

where,

$\hat{y}$ is the final predicted value
k is the number of nearest neighbors
y_i are the actual target values of the k closest neighbors.

The model performance is evaluated by minimizing the MSE.

3.7.6 Huber Regressor

Huber Regressor is a robust regression technique used in machine learning to handle data with outliers. It combines the properties of both ordinary least squares regression and mean absolute error regression, making it less sensitive to outliers than standard linear regression. The Huber Regressor minimizes the Huber loss function, which is defined as:

$$L_\delta(a) = \begin{cases} \frac{1}{2}a^2 & for\ |a| < \delta \\ \delta\left(|a| - \frac{1}{2}\delta\right) & for\ |a| > \delta \end{cases} \quad (6)$$

where, a is the residual (difference between the observed and predicted values), and δ is a threshold parameter. For residuals smaller than δ, the Huber loss behaves like the squared loss, and for larger residuals, it behaves like the absolute loss. The Huber Regressor iteratively optimizes the loss function to find the best-fitting model. This involves solving a convex optimization problem, which ensures convergence to a global minimum.

Chapter 4. Results and Discussions

4.1 Analysis of TSD Data

As mentioned in the previous section, a comprehensive set of pavement condition indicators including Surface Curvature Index (SCI), Base Curvature Index (BCI), Area Under Pavement Profile (AUPP) and D1500 were determined from TSD data to determine the pavement conditions of I-35 SB, I-40 EB and I-40 WB segments. For this purpose, the raw TSD data was first processed and cleaned to remove any anomalous data and empty cells. The TSD deflection basin parameters were then calculated from the cleaned TSD data. These basin parameters were then used to categorize pavement sections of I-35 SB, I-40 EB and I-40 WB in good, fair and poor conditions using the thresholds mentioned in Table 5.

4.1.1 Surface Curvature Index (SCI300)

Figures 15(a), 15(b) and 15(c) show the variation of SCI300 values for I-35 SB, I-40 EB and I-40 WB, respectively. As mentioned in the literature review, the SCI300 index represents the structural conditions of the surface layer of the pavements. A lower value of SCI300 typically represents higher strength of the surface layer. From Figures 15(a), 15(b) and 15(c), it was observed that the I-35 SB segments show relatively lower SCI300 values than the I-40 EB and I-40 WB segments. After consulting with District 4 personnel, it was found that the I-40 EB and I-40 WB are mostly flexible pavements, whereas the I-35 segments have composite pavement sections made of concrete over asphalt. As a result, higher SCI300 values are expected for the I-35 segments.

Virginia Tech Transportation Institute uses the SCI300 index to categorize pavement conditions (Katicha et al., 2020). According to them, the pavement sections with SCI300 values of less than 68.58 μm, between 68.58 to 93.98 μm and more than 93.98 μm can be categorized as good, fair and poor conditioned, respectively. In this current study, these thresholds were used for characterization of the tested I-35 SB, I-40 EB and I-40 WB segments, as indicated in Table 5. These threshold limits are shown in Figures 15(a), 15(b) and 15(c) to identify the good, fair and poor pavement sections of I-35 SB, I-40 EB and I-40 WB, respectively. It was observed that most of the I-35 sections were categorized as good conditioned. The composite pavement layers may be responsible for this phenomenon. From Figures 15(b) and 15(c), many of the I-40 EB and I-40 WB sections fall under fair to poor categories.

4.1.2 Base Curvature Index (BCI)

The Base Curvature Index or BCI is an indicator of the condition of the lower structural layers like base and subgrade layers. Figures 16(a), 16(b) and 16(c) present the variation of BCI indices for I-35 SB, I-40 EB and I-40 WB segments, respectively. Similar to SCI300, a lower value of BCI represents higher strength of the lower structural layers. From Figures 16(a), 16(b) and 16(c), it was observed that the I-35 SB and I-40 EB segments have lower BCI values than the I-40 WB. According to TxDOT (Chang et al., 2014), a BCI value of less than 76.02 μm represents a good pavement condition. A pavement section with a BCI value higher than 76.02 μm but less than 101.6 μm can be treated as fair and more than 101.6 μm as poor conditions. Figures 16(a), 16(b) and 16(c) show the good, fair and poor pavement sections of I-35 SB, I-40 EB and I-40 WB, respectively, based on BCI value. It was observed that almost all of I-35 SB and I-40 EB have BCI values less than 76.02 μm, representing good conditions of the pavements. Some sections of I-40 WB were found to exhibit fair conditions.

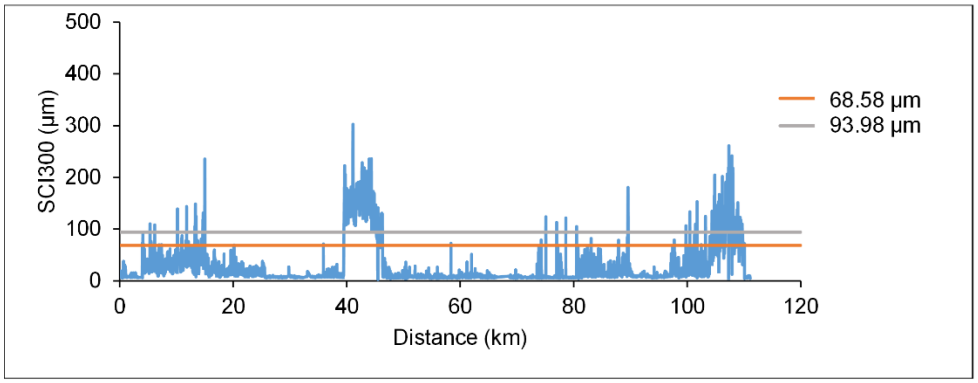

(a)

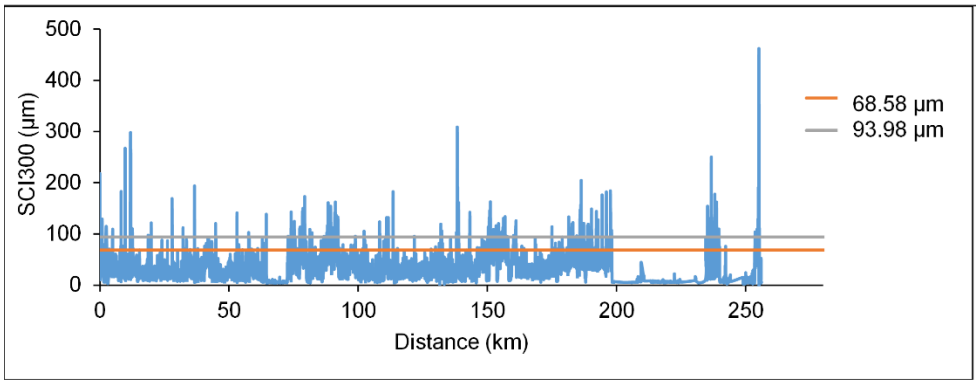

(b)

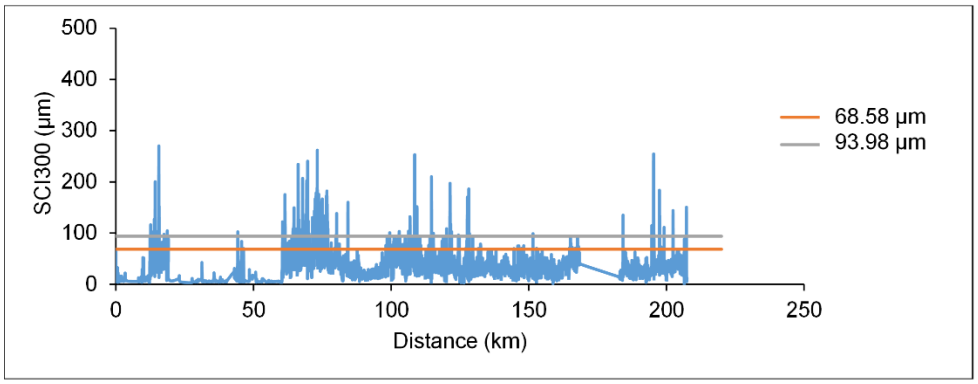

(c)

Figure 15 Variation of SCI300 index for (a) I-35 SB, (b) I-40 EB and (c) I-40 WB segments.

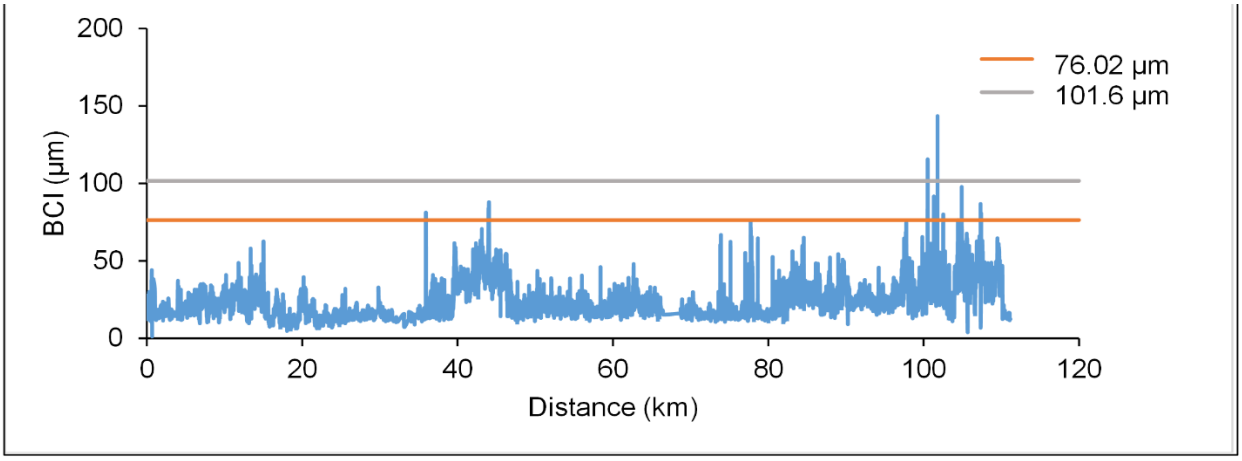

(a)

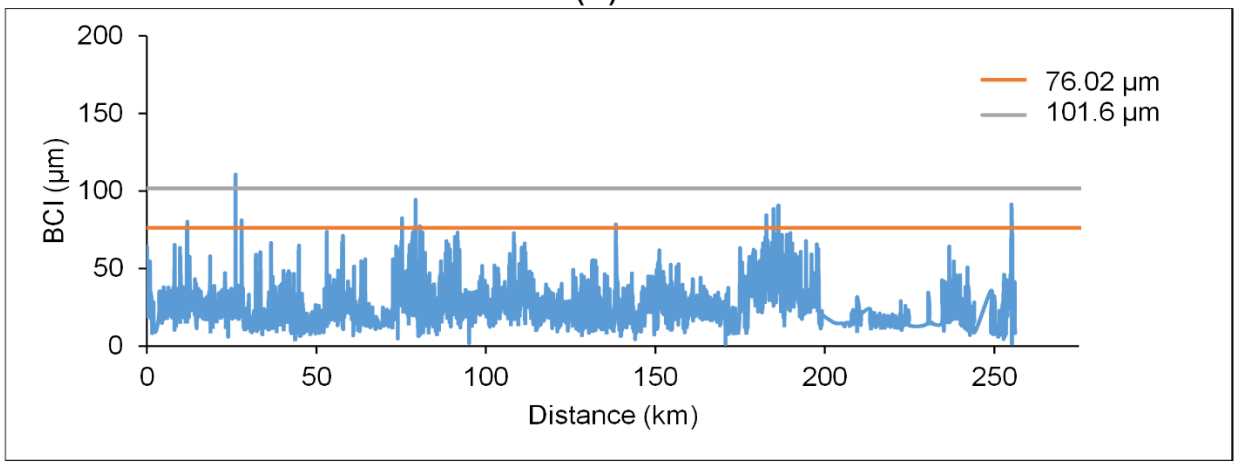

(b)

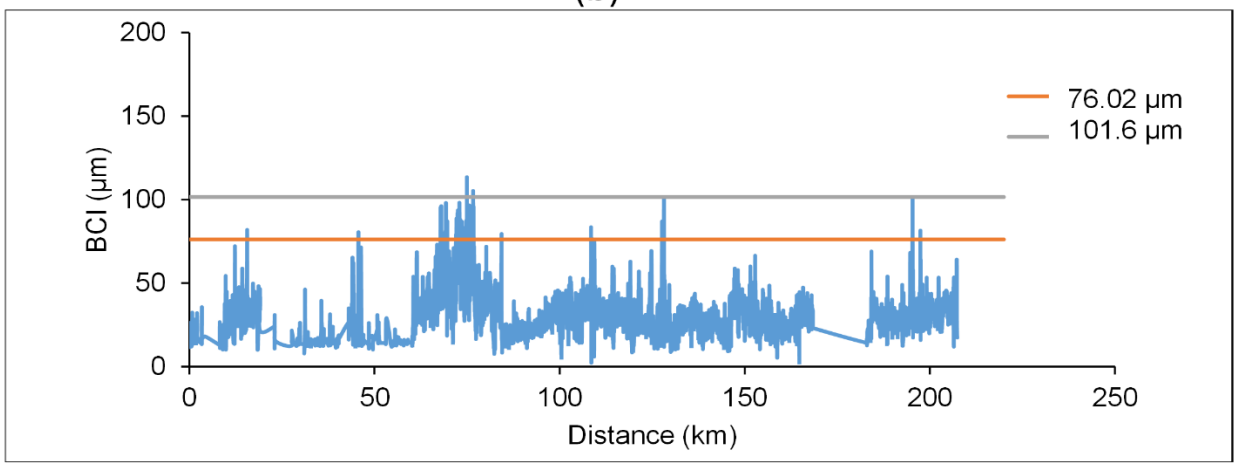

(c)

Figure 16 Variation of BCI index for (a) I-35 SB, (b) I-40 EB and (c) I-40 WB segments.

4.1.3 D1500

Figures 17(a), 17(b) and 17(c) show the variation of D1500 values for I-35 SB, I-40 EB and I-40 WB, respectively. As mentioned in the literature, the D1500 index shows the conditions of the subgrade layer of a pavement. A lower value of D1500 represents better condition of the subgrade layer. It was observed that the I-35 SB, I-40 EB and I-40 WB segments showed almost similar ranges of D1500 values. Tennessee DOT (TDOT, 2024) indicated that pavement sections with a D1500 value of less than 25.4 µm can be considered as good whereas more than 55.88 µm can be treated as poor. The sections with a D1500 value of more than 25.4 µm but less than 55.88 µm should be categorized as fair condition. It was observed that most of the I-35 SB, I-40 EB and I-40 WB sections fell under good to fair conditions, indicating strong subgrade layers.

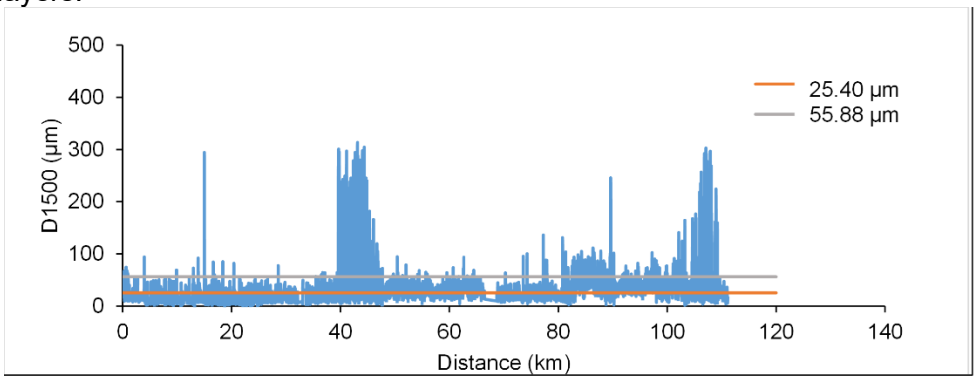

(a)

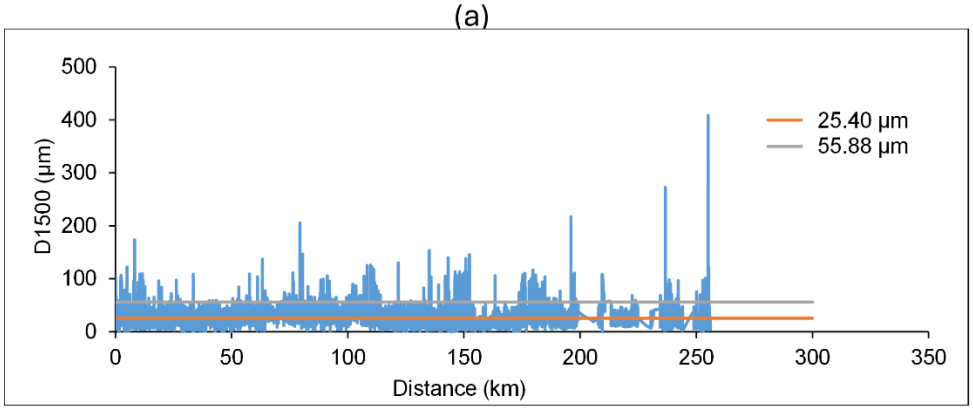

(b)

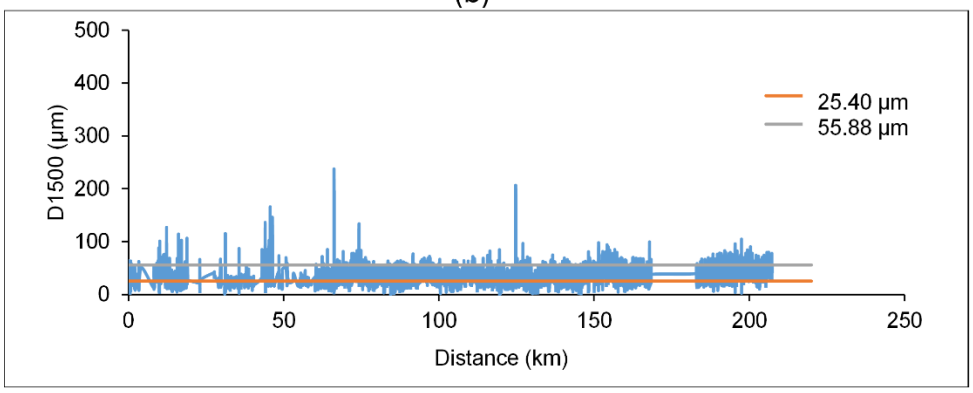

(c)

Figure 17 Variation of D1500 index for (a) I-35 SB, (b) I-40 EB and (c) I-40 WB segments.

4.1.4 Area Under Pavement Profile (AUPP)

The Area Under Pavement Profile (AUPP) index indicates the characteristics of the upper layers of the pavement. Figures 18(a), 18(b) and 18(c) show the variation of AUPP values for I-35 SB, I-40 EB and I-40 WB, respectively. A lower value of AUPP indicates higher strength of the pavement layers. From Figures 18(a), 18(b) and 18(c), it was observed that the I-35 SB, I-40 EB and I-40 WB segments showed almost similar ranges of AUPP indices.

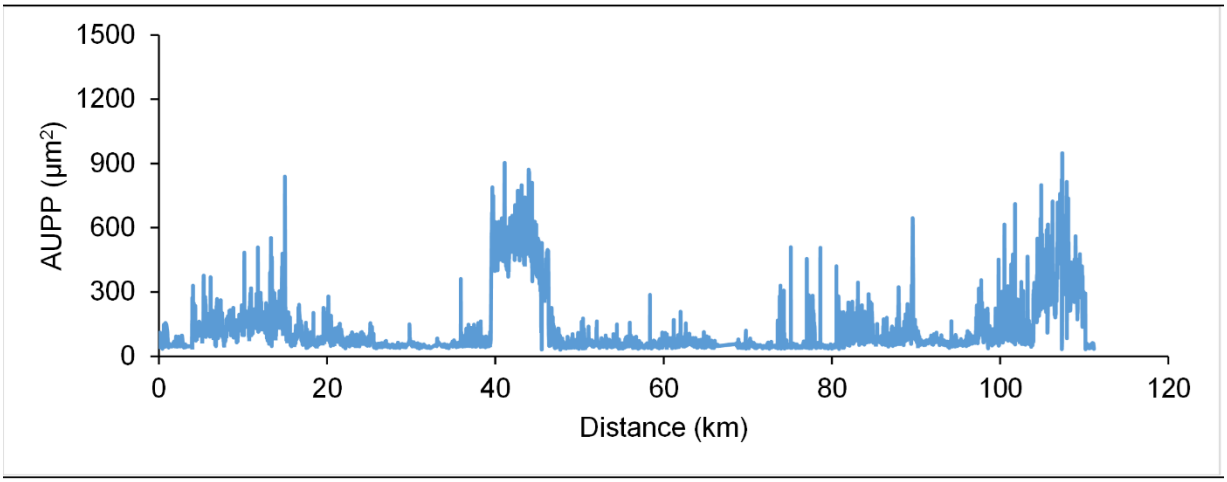

(a)

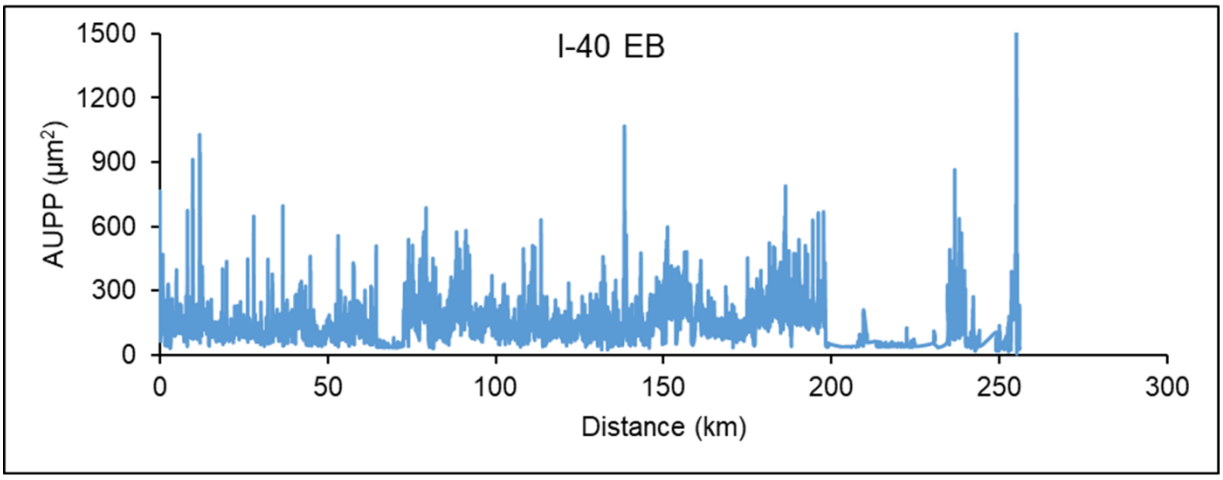

(b)

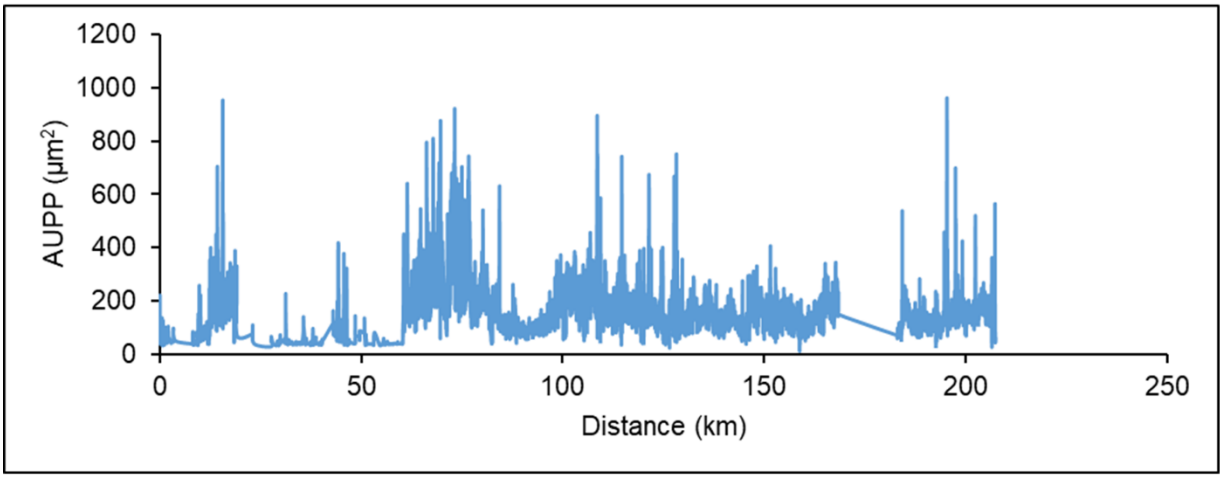

(c)

Figure 18 Variation of AUPP index for (a) I-35 SB, (b) I-40 EB and (c) I-40 WB segments.

4.2 Selection of Experimental Sites

As mentioned in the previous section, the threshold limits mentioned in Table 5 for SCI300, BCI and D1500 were used for the initial categorization of the I-35 SB, I-40 EB and I-40 WB into good, fair and poor conditions. The details of this categorization were presented in the previous sections. Based on this categorization, the team identified three experimental sites to represent three pavement categories, namely poor, fair, and good from I-35, each spanning a length of 10 to 15 kilometers. The idea was to select a stretch of a highway section that mostly represents a specific category based on all the TSD indices at network-level. Similarly, another three experimental sites were selected from I-40 (combining I-40 EB and I-40 WB). The approximate locations of the I-35 and I-40 experimental sites are presented in Figures 19(a) and 19(b), respectively. As mentioned in Figure 19(a), Section 1, Section 2 and Section 3 of I-35 represent fair, good and poor conditions, respectively. From Figure 19(b), on I-40, Section 1, Section 2 and Section 3 represent poor, good and fair conditions, respectively. These experimental sites were then used for further evaluation using FFWD, GPR, Pave3D 8K and coring.

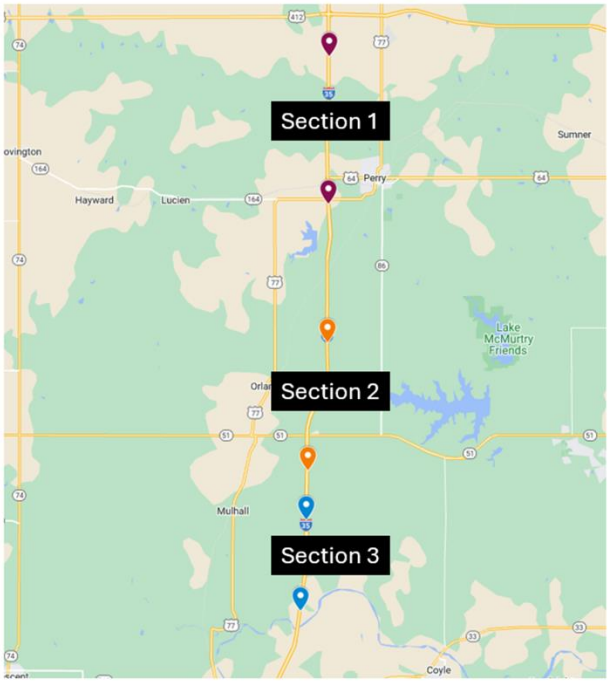

(a)

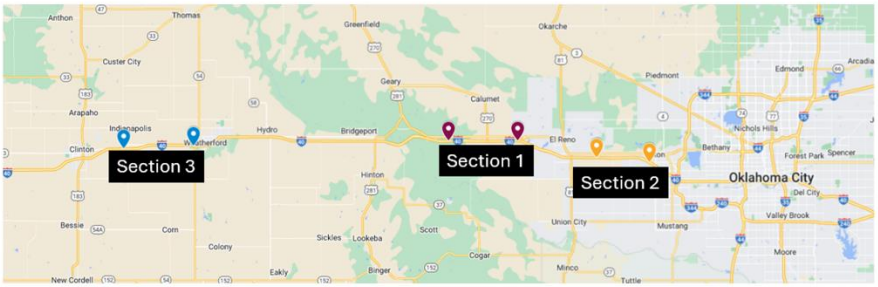

(b)

Figure 19 Selection of Experimental Sites for Evaluation: (a) I-35, and (b) I-40

4.3 Pave3D 8K Measurements

Pavement surface conditions of the experimental sites identified using TSD analysis were assessed using the Pave3D 8K. As mentioned earlier, Pave3D 8K data was collected and analyzed by the OSU team. In this study, four different pavement parameters were selected for evaluating the conditions of the experimental sites. These parameters include rut depth, texture parameters including Mean Profile Depth (MPD), and percentage (%) of cracks on the wheel path and non-wheel paths.

4.3.1 Comparison of I-35 Experimental Sites:

Figures 20, 21, 22 and 23 show the rut depth, Mean Profile Depth (MPD), %cracking on the wheel path and %cracking on the non-wheel paths for I-35 experimental sites, respectively. From Figures 20(a), 20(b) and 20(c), it was observed that the rut depths varied from 0.35-5.35 mm, 0.45-2.46 mm, 0.4-10 mm for I-35 Section 1, Section 2 and Section 3, respectively. These results match with TSD analysis as I-35 Section 1, Section 2 and Section 3 were rated as fair, good and poor conditioned, respectively.

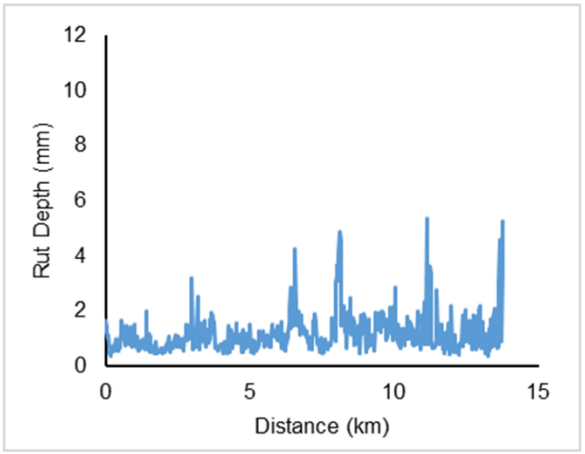

(a)

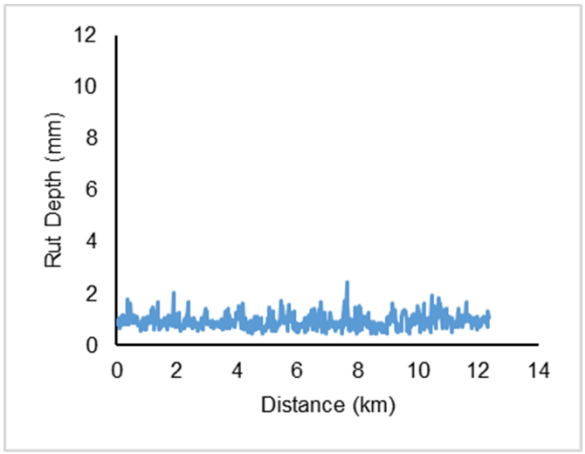

(b)

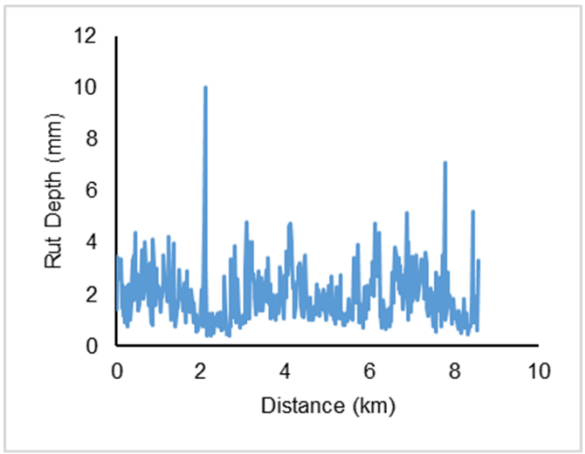

(c)

Figure 20 Rut depth of I-35 experimental sites: (a) Section 1 (fair), (b) Section 2 (good) and (c) Section 3 (poor)

As shown in Figures 21(a), the MPD for I-35 Section 1 was found to vary from 0.8-1.8 mm with an average of 1.0 mm. The MPD for I-35 Section 2 varied between 0.7-1.9 mm with an average of 0.9 mm and I-35 Section 3 varied between 0.7-3.5 mm with an average of 1.3 mm. Generally, a higher value of MPD indicates better resistance to skid and improved pavement conditions. Therefore, the MPD results do not match the TSD results.

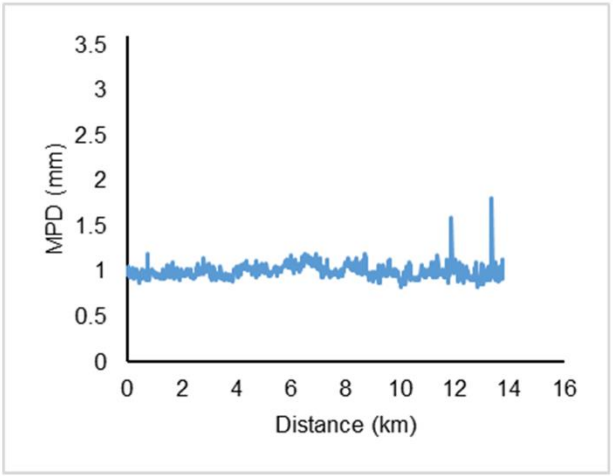

(a)

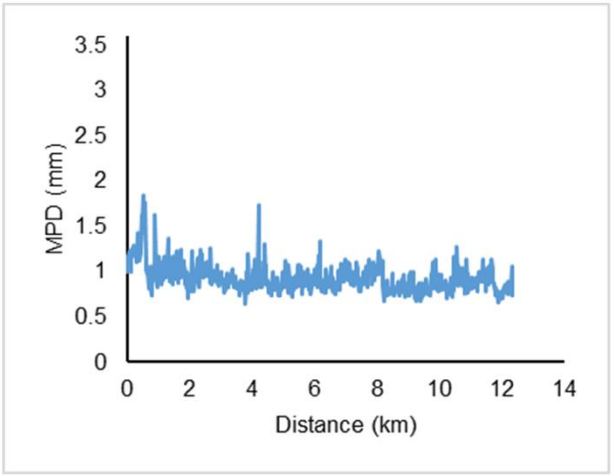

(b)

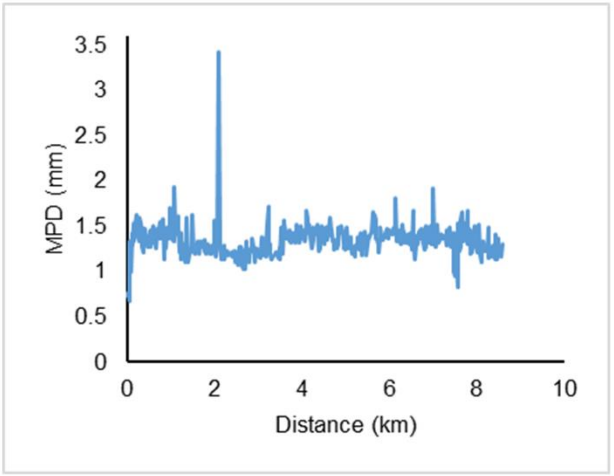

(c)

Figure 21 Mean Profile Depths of I-35 experimental sites: (a) Section 1 (fair), (b) Section 2 (good) and (c) Section 3 (poor)

The cracks on the wheel path typically occur from the passing of traffic and are often referred to as the load-related cracking. A lower value of %cracking refers to better condition of the pavement. From Figures 22(a), 22(b) and 22(c), the %cracking on the wheel path was found to vary between different experimental sites. The %cracking on the wheel path for I-35 Section 1 ranged from 0% to1.6% with an average of 0.1%. The I-35 Section 2 also exhibited similar results of %cracking on the wheel path with an average of 0.3%. The I-35 Section 3 exhibited the highest cracking among the three sections with an average of 1.9%. The results indicate almost similar conditions for the good (Section 2) and fair (Section 1) sections. The Section 3, which was identified as poor from TSD analysis, was found to exhibit higher cracking on the wheel path from Paave3D 8k analysis.

The cracking on the non-wheel path is mostly related to the environmental loading on the pavement section. It was found that the %cracking on the non-wheel path of Section 1, Section 2 and Section 3 varied from 0-1.7%, 0-2.2% and 0-4.4%, respectively (Figures 23(a), 23(b) and 23(c)). Therefore, the %cracking on the non-wheel path from Pave3D 8K are in agreement with the TSD results.

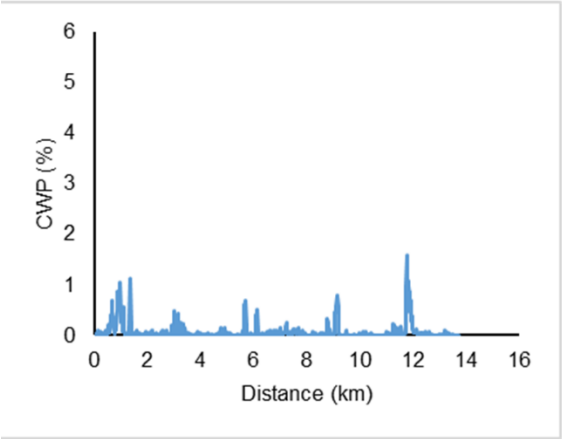

(a)

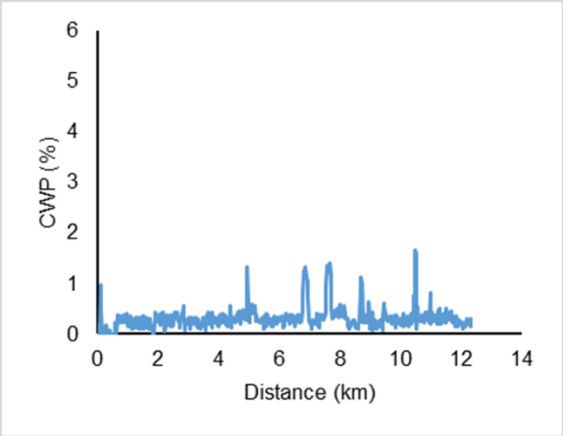

(b)

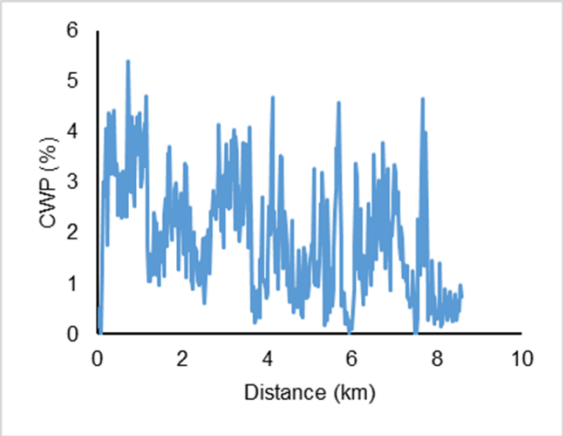

(c)

Figure 22 %Cracking on the wheel path of I-35 experimental sites: (a) Section 1 (fair), (b) Section 2 (good) and (c) Section 3 (poor)

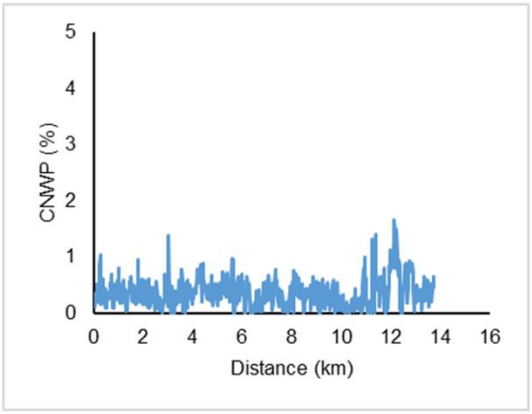

(a)

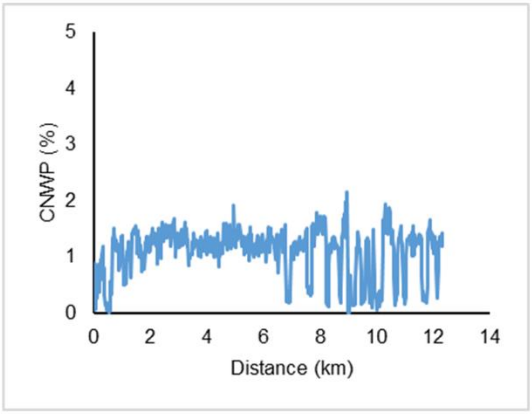

(b)

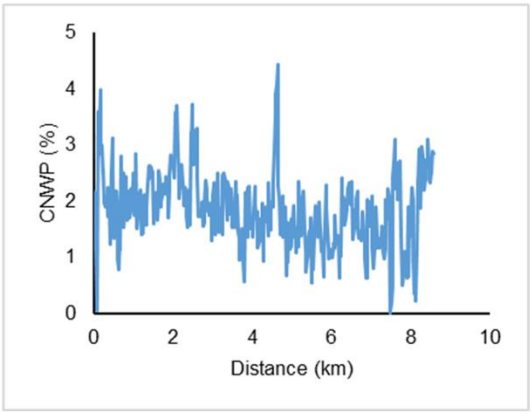

(c)

Figure 23 %Cracking on the non-wheel path of I-35 experimental sites: (a) Section 1 (fair), (b) Section 2 (good) and (c) Section 3 (poor)

4.3.2 Comparisons of I-40 Experimental Sites

Figures 24(a), 24(b) and 24(c) show the rut depths for I-40 Section 1, Section 2 and Section 3, respectively. From Figures 24(a), the average rut depths for I-40 Section 1 were found to be 1.14 mm with values ranges from 0.4 mm to 6.0 mm. The I-40 Section 2 exhibited lesser rut depths than I-40 Section 1 with an average of 1.1 mm. The average rut depths for I-40 Section 3 were found to be 2.0 mm, respectively. The results indicate that the I-40 Section 1 can be categorized as the better performing section among the three sections which is in agreement with the TSD analysis. The ranking of the I-40 Section 2 and 3 does not match with TSD analysis.

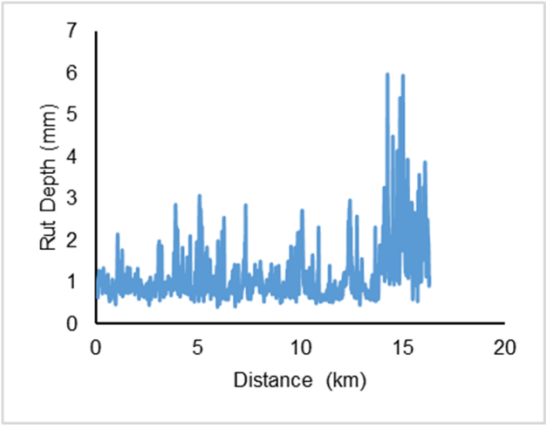

(a)

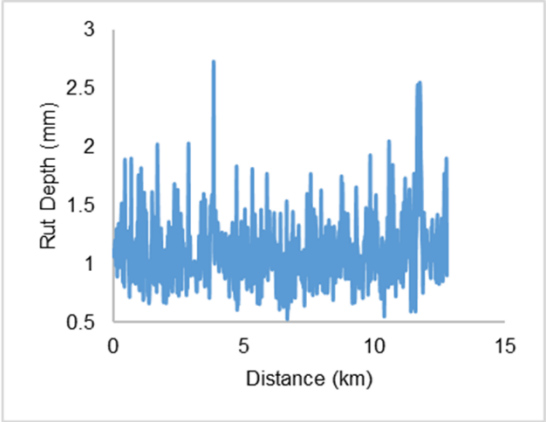

(b)

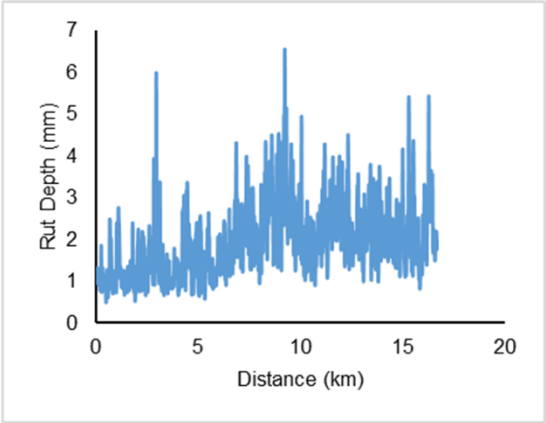

(c)

Figure 24 Rut depth of I-40 experimental sites: (a) Section 1 (poor), (b) Section 2 (good) and (c) Section 3 (fair)

From Figures 25(a), the average values for MPD for Section 1, Section 2 and Section 3 were observed to be 1.6 mm, 0.8 mm and 2.1 mm, respectively. Therefore, the MPD results do not

expect to provide the same pavement categorization as the TSD results for I-40 experimental sites.

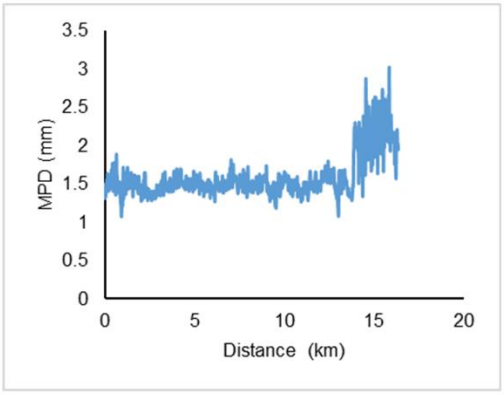

(a)

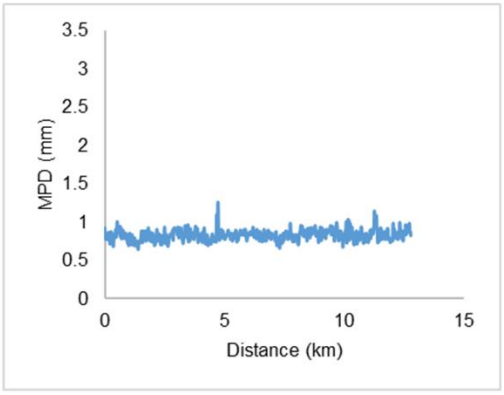

(b)

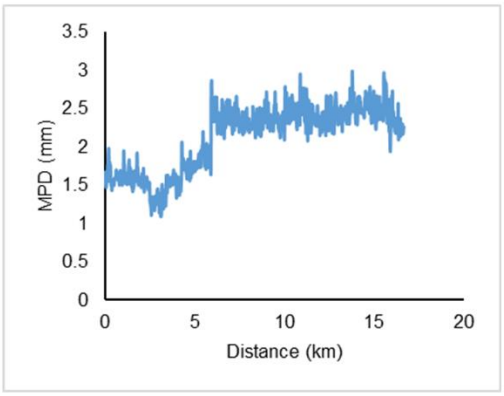

(c)

Figure 25 Mean rut depths of I-40 experimental sites: (a) Section 1 (poor), (b) Section 2 (good) and (c) Section 3 (fair)

The %cracking on the wheel path and non-wheel path showed similar trends as seen from Figures 26 and 27. From Figures 26(a), 26(b) and 26(c), the %cracking on the wheel path was found to vary from 0-1.8%, 0-1.5%, and 0-1.7% for I-40 Section 1, Section 2 and Section 3, respectively. The average %cracking on the wheel path for I-40 Section 1, Section 2 and Section 3 were 0.1%, 0.3% and 0.1%. Similar trends were observed from Figures 27(a), 27(b) and 27(c) for cracking on the non-wheel path. The results show that the pavement conditions across all I-40 experimental sites are nearly identical, making it challenging to differentiate between them. The findings suggest that classifying pavements based solely on structural or functional characteristics can sometimes be misleading. Therefore, an integrated categorization that considers both structural and functional aspects is essential for the effective management of pavement infrastructure systems.

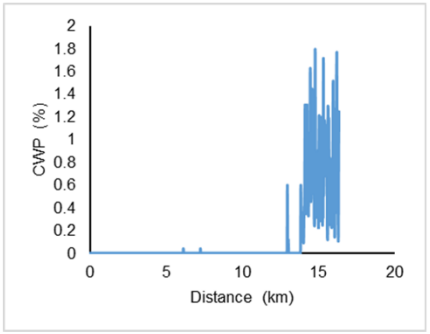

(a)

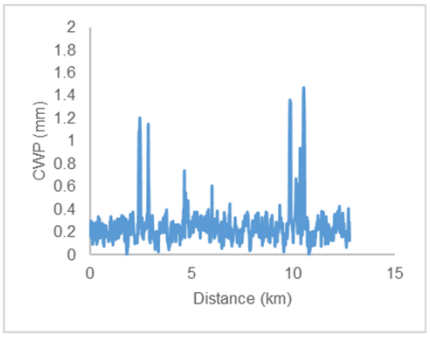

(b)

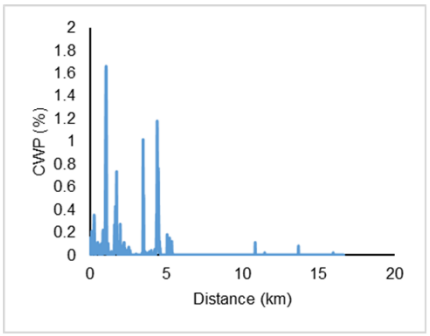

(c)

Figure 26 %Cracking on wheel path of I-40 experimental sites: (a) Section 1 (poor), (b) Section 2 (good) and (c) Section 3 (fair)

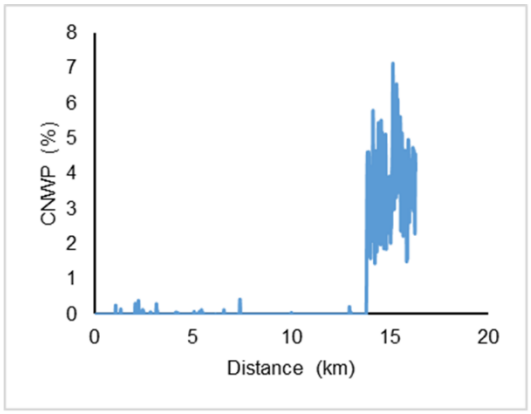

(a)

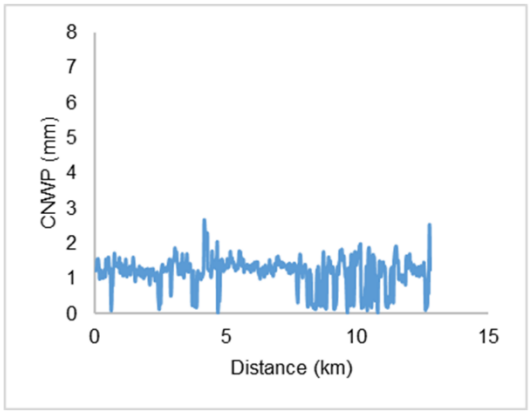

(b)

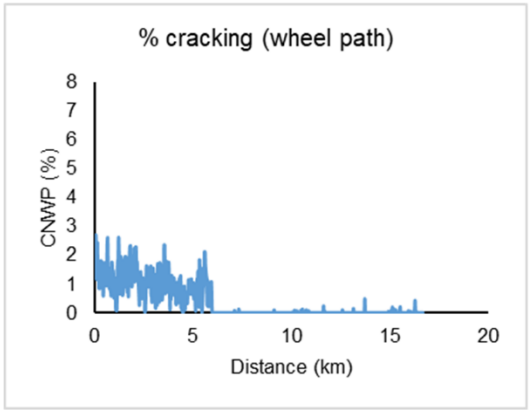

(c)

Figure 27 %Cracking on non-wheel path of I-40 experimental sites: (a) Section 1 (poor), (b) Section 2 (good) and (c) Section 3 (fair)

4.4 Physical Inspection of Field Cores

As mentioned earlier, the OU team collected field cores selectively from the I-35 experimental sites. These cores were physically inspected to measure the pavement thickness and to observe any visible damage. Figures 28(a), 28(b) and 28(c) show the extracted cores from the I-35 Section 1, Section 2 and Section 3, respectively. Detailed observations were documented and are presented in Table 6. From Table 6, the I-35 Section 2 was found to be a composite pavement made of approximately 9 inch (230 mm) thick concrete over 6 inch (150 mm) of asphalt layers. As a result, this section showed less deflection and was ranked as good conditioned from TSD analysis. The I-35 Section 1 was found to be made of 9-10 inch thick asphalt layers with hot sand as base materials. Most of the cores from I-35 Section 3 broke during coring operation and could not be recovered. It was found that this section contained approximately 8 inch of asphalt. As I-35 Section 1 and 3 were made of asphalt materials, it was expected that these sections would show inferior pavement conditions than I-35 Section 2. From plan notes, it was found that most of the I-40 sections were flexible pavements. The thickness of the asphalt layers of I-40 was found to be approximately 10 inches.

Figure 28 Physical inspection of roadway cores from I-35 (a) Section 1, (b) Section 2 and (c) Section 3

Table 6 Properties of the roadway cores

ID	L1 (mm)	L2 (mm)	L3 (mm)	L4 (mm)	L5 (mm)	Total (mm) Calculated	L1 Type	L2 Type	L3 Type	L4 Type	L5 Type	Notes
A1	95.12	Broken				95.12	S4					
A2	90.74	Broken				90.74	S4	S4				
A3	46.27	52.39	Broken			98.66	S4	S4	S4			L3 Fabric
A4	50.65	45.66	29.90	Broken		126.22	S4	S4	S4			L3 Broken
A5	49.10	55.14	51.32	79.59	11.95	235.15	S4	S4	S5	S5	S3	Fabric Between Lifts
A6	42.89	42.42	25.01	35.19	82.49	228.00	S4	S4	S5	S5	S3	L3 Fabric
B1	222.12	28.20	31.75	72.38	69.62	354.45	PCC	S5	S5	S2	BBC AT	L2/L3 Delaminated
B2	224.09	Broken				224.09	PCC					
B3	223.95	42.56	29.09	76.60		372.20	PCC	HMA	HMA	HMA		
C1	66.58	53.60	93.47			213.65	S4	S4	S3			
C2	75.39	53.23	86.91	40.71		256.25	S4	S4	S3	S2		
C3	72.82	51.15	89.43	38.62		252.01	S4	S4	S3	S2		
C4	67.57	61.53	88.39	38.81		256.30	S4	S4	S3	S2		
C5	61.16	68.60	97.90			227.66	S4	S3	S2			
C6	70.99	60.49	102.56			234.04	S4	S4	S3			

4.5 Roadway Profile using Face Dipstick

Rut depths and roadway profiles were measured on the selected places of I-35 Section 1, Section 2 and Section 3 using the Face Dipstick. Table 7 shows the summary of road profiles from Face Dipstick measurements. Rut depths of the I-35 Section 2 were found to vary from 0.038 to 0.108 inch. The I-35 Section 1 and Section 3 were found to show rut depths of 0.093-0.393 in. and 0.026-0.332 in., respectively. The pavement categorization using rut depths from Face Dipstick matches with the ranking obtained from the TSD analysis.

Table 7 Rut Depths from Face Dipstick

Test Section	ID	Rut Depth in Left Wheel Path(in)	Rut Depth in Right Wheel Path (in)
I-35 Section 1	A1	-0.102	-0.093
I-35 Section 1	A2	-0.168	-0.124
I-35 Section 1	A3	-0.151	-0.102
I-35 Section 1	A4	-0.137	-0.393
I-35 Section 1	A5	-0.155	-0.099
I-35 Section 1	A6	-0.139	-0.138
I-35 Section 2	B1	-0.097	-0.130
I-35 Section 2	B2	-0.104	-0.017
I-35 Section 2	B3	-0.108	-0.038
I-35 Section 3	C1	-0.327	-0.107
I-35 Section 3	C2	-0.093	-0.209
I-35 Section 3	C3	-0.076	-0.026
I-35 Section 3	C4	-0.233	-0.014
I-35 Section 3	C5	-0.038	-0.222
I-35 Section 3	C6	-0.043	-0.332

4.6 Structural Evaluation using FFWD

As previously mentioned, FFWD tests were conducted by the TTI team on the selected experimental sites for determining the structural capacity of the pavement sections. During this test, impact loads were applied to the pavement surface and the pavement responses (vertical deflections) were measured using a series of geophone sensors (W1 to W7). The FFWD test data were analyzed using the MODULUS 7.0 software (a back-calculation program for analyzing FWD data). In addition to normalized deflection (with respect to 9-kip load), the software can provide layer moduli. A snippet of the FFWD processed data of the I-35 Section 1 is presented in Figure 29. In this study, the normalized (9-kip) deflections of W1, W6 and W7 sensors and elastic modulus of the surface layer obtained from the FFWD tests were used for the evaluation of the structural conditions of the experimental sites.

No.	Station (mi)	LANE	Longitude	Latitude	Load	W1	W2	W3	W4	W5	W6	W7
7	0.0		-97.327174	36.371828	8533	10.62	5.21	3.00	2.11	1.47	1.24	0.96
8	0.1		-97.327169	36.370314	8687	9.49	4.88	2.52	1.67	1.15	0.86	0.70
9	0.2		-97.327163	36.368966	8687	8.31	3.70	2.33	1.66	1.13	0.79	0.57
10	0.3		-97.327158	36.367536	8599	10.83	5.06	3.23	2.43	1.78	1.38	1.14
11	0.4		-97.327149	36.366047	8676	11.54	5.55	3.30	2.40	1.74	1.31	1.04
12	0.5		-97.327149	36.364571	8424	13.98	5.30	3.42	2.61	1.94	1.44	1.10
13	0.6		-97.327141	36.363111	8391	14.84	6.13	2.89	2.15	1.61	1.28	1.06
14	0.7		-97.327137	36.361542	8566	11.82	5.22	3.08	2.28	1.76	1.40	1.09
15	0.8		-97.327131	36.360326	8512	13.67	7.30	4.13	2.76	1.83	1.39	1.09
16	0.9		-97.327128	36.358845	8457	18.31	6.15	2.50	1.72	1.23	0.91	0.72
17	1.0		-97.327124	36.357358	8643	10.57	5.00	3.28	2.48	1.85	1.47	1.19
18	1.1		-97.327120	36.355871	8413	15.70	6.84	4.36	3.30	2.50	1.93	1.47
19	1.2		-97.327115	36.354483	8687	9.94	5.38	3.59	2.66	1.97	1.49	1.14

Figure 29 Snippet of FFWD Data of I-35

4.6.1 Comparisons of I-35 Experimental Sites

The variations in normalized (9-kip) deflections of W1, W6 and W7 sensors of I-35 experimental sites are presented in Figures 30(a), 30(b) and 30(c), respectively. A clear trend for distinguishing the good, fair and poor sites was observed from the normalized deflection of W1 sensor as evident from Figure 30(a). The average values of the normalized W1 deflections were found to be 3.5, 12.6 and 14.9-mil, for good (Section 2), fair (Section 1) and poor (Section 3) experimental sites, respectively. According to Chen et al. (2003), any pavement section with a normalized W1 deflection of less than 10-mill can be considered as structurally adequate. Therefore, at network-level, fair (Section 1) and poor (Section 3) I-35 experimental sites could be considered structurally inadequate. From Figures 30(b) and 30(c), no proper trend of normalized W6 and W7 deflections were observed to distinguish between different pavement categories.

Variation of the surface modulus (E1) of the I-35 experimental sites are presented in Figure 30(d). The average values of the E1 for good (Section 2), fair (Section 1) and poor (Section 3) sections of I-35 were found as 4027, 94 and 76-ksi, respectively. Generally, any pavement section with a surface layer modulus less than 145-ksi (1,000 MPa) is classified as poor, 145-435 ksi (1,000-3,000 MPa) as moderate (fair) and more than 435 ksi (3,000 MPa) as a strong (good) pavement (ARA 2004, Huang 2004; Khazanovich & Tayabji 2007). Therefore, the FFWD evaluations classified both poor and fair sections as poor sections. The results indicates that the pavement rankings obtained from W1 deflection and E1 modulus are similar to TSD classifications.

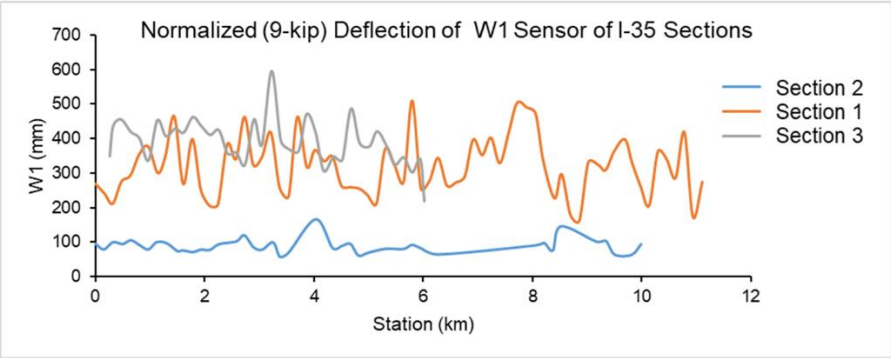

(a)

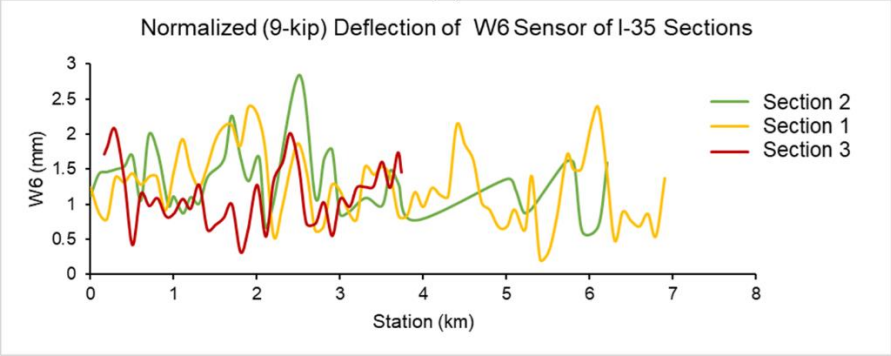

(b)

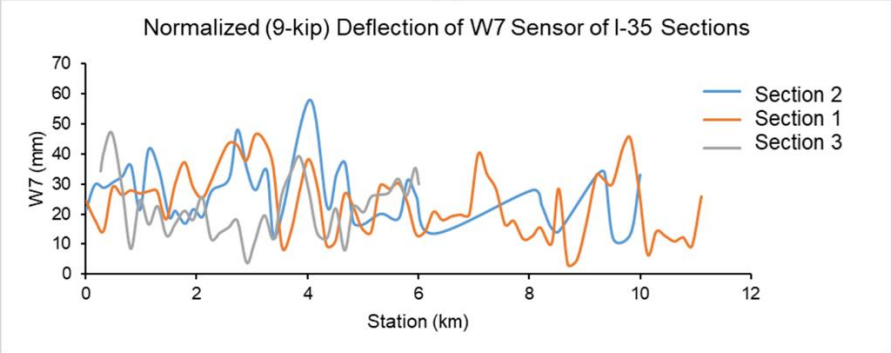

(c)

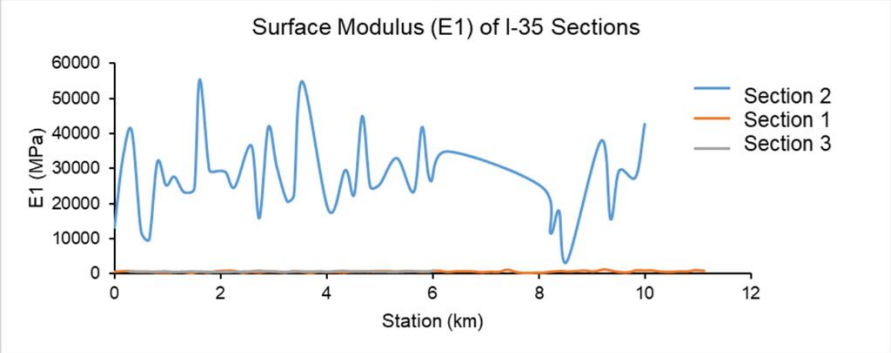

(d)

Figure 30 FFWD Structural Response Parameters of I-35 Test Sections: (a) Deflection of W1 Sensor; (b) Deflection of W6 Sensor; (c) Deflection of W7 Sensor; and (d) Surface Modulus (E1)

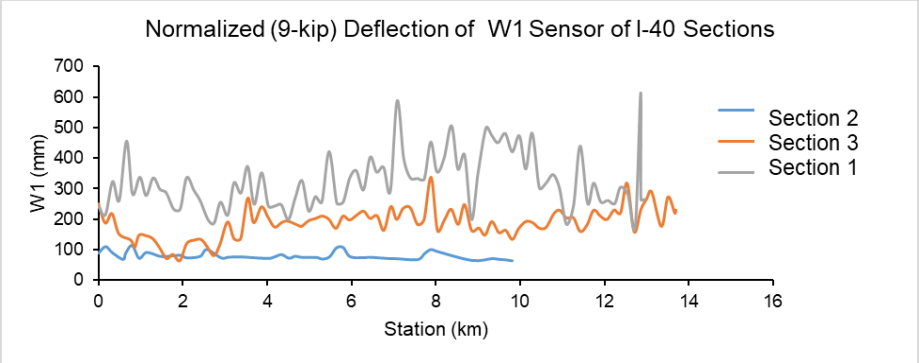

(a)

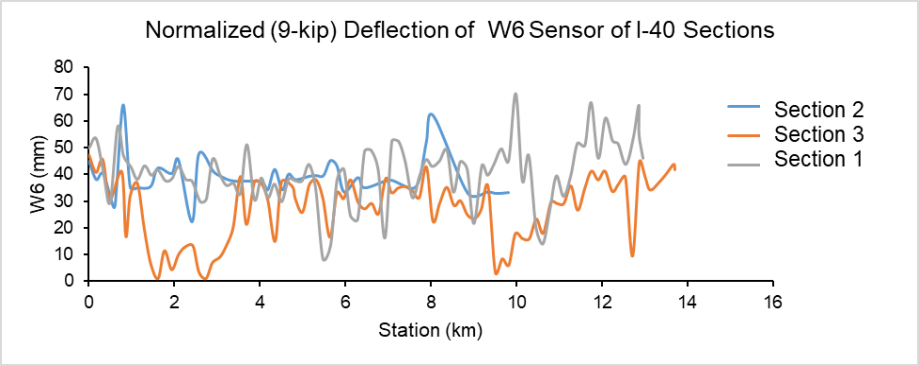

(b)

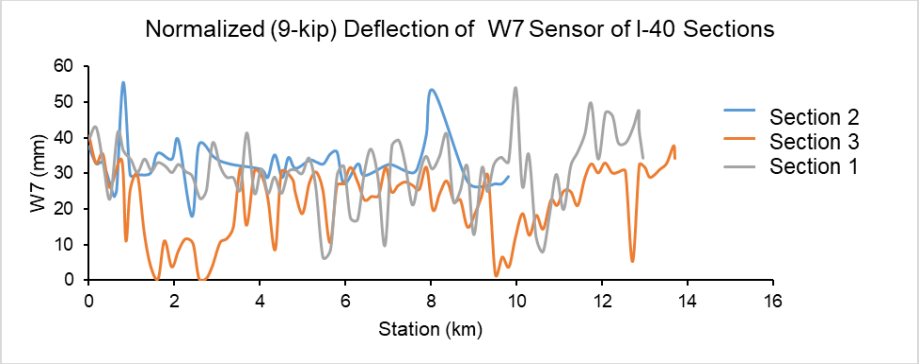

(c)

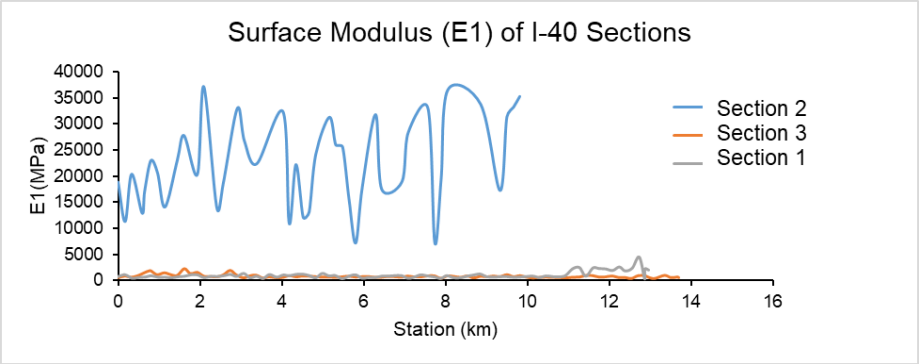

(d)

Figure 31 FFWD Structural Response Parameters of I-40 Test Sections: (a) Deflection of W1 Sensor; (b) Deflection of W6 Sensor; (c) Deflection of W7 Sensor; and (d) Surface Modulus (E1)

4.6.2 Comparisons of I-40 Experimental Sites

Figures 31(a), 31(b) and 31(c) presents the variations of normalized W1, W6 and W7 deflections of I-40 experimental sites, respectively. The results of the normalized W1, W6 and W7 deflections of I-40 experimental sites were found to be similar as I-35 experimental sites. The average values of the normalized W1 deflections of I-40 experimental sites were found to be 3.20, 7.35 and 12.72-mil, for good (Section 2), fair (Section 3) and poor (Section 1) conditions, respectively. In this case, only I-40 Section 1 showed a normalized W1 deflection higher than 10-mil which was already identified to have poor structural condition. No proper trend was observed for W6 and W7 deflections as evident from Figures 31(b) and 31(c). The E1 values of the I-40 experimental sites are shown in Figure 31(d). The average values of the E1 were found to be 3,263, 117 and 148-ksi, for good (Section 2), fair (Section 3) and poor (Section 1) experimental sites, respectively. Although the poor section exhibited a higher average E1 value than the fair section, the difference is not significant. According to current literature (ARA 2004, Huang 2004; Khazanovich & Tayabji 2007), both fair (Section 3) and poor (Section 1) experimental sites can be classified as structurally poor conditioned.

4.7 Pavement Condition Evaluation Using GPR

In this study, the pavement structures of selected experimental sites of I-35 and I-40 were surveyed using the TTI's air coupled-GPR. During this survey, the dielectric values of the subsurface were collected and then analyzed to evaluate pavement conditions. The TTI team helped analyze the collected data. GPR facilitated continuous measurements of pavement thicknesses in these test sites. This data was further calibrated using field cores. Also, the subsurface conditions and defects, such as voids and anomaly were identified from the GPR measurements. Figure 32 shows a screenshot of the GPR data analysis window. In this study, a qualitative analysis was performed to compare GPR images with TSD data at network-level.

Figure 32 Screenshot of the GPR data analysis window

4.7.1 GPR Images of I-35 Experimental Sites:

Figures 33(a), 33(b) and 33(c) present the snippets of GPR images obtained from I-35 Section 1, Section 2 and Section 3, respectively. From Figure 33(a), disturbance in the subsurface can be seen at several locations of I-35 Section 1. The areas of disturbance are marked with red boxes. Some disturbance were expected as I-35 Section 1 was rated as fair conditioned. From Figure 33(b), although the initial stretch of I-35 Section 2 exhibited some disturbances, the rest of the pavement was found to show good subsurface conditions. This result is in agreement with TSD data as the I-35 Section 2 was categorized as good conditioned. The I-35 Section 3 was

rated as poor conditioned from TSD analysis and was found to have subsurface distresses at many locations, as shown in Figure 33(c). Therefore, the ranking from TSD analysis was found to be in agreement with GPR analysis.

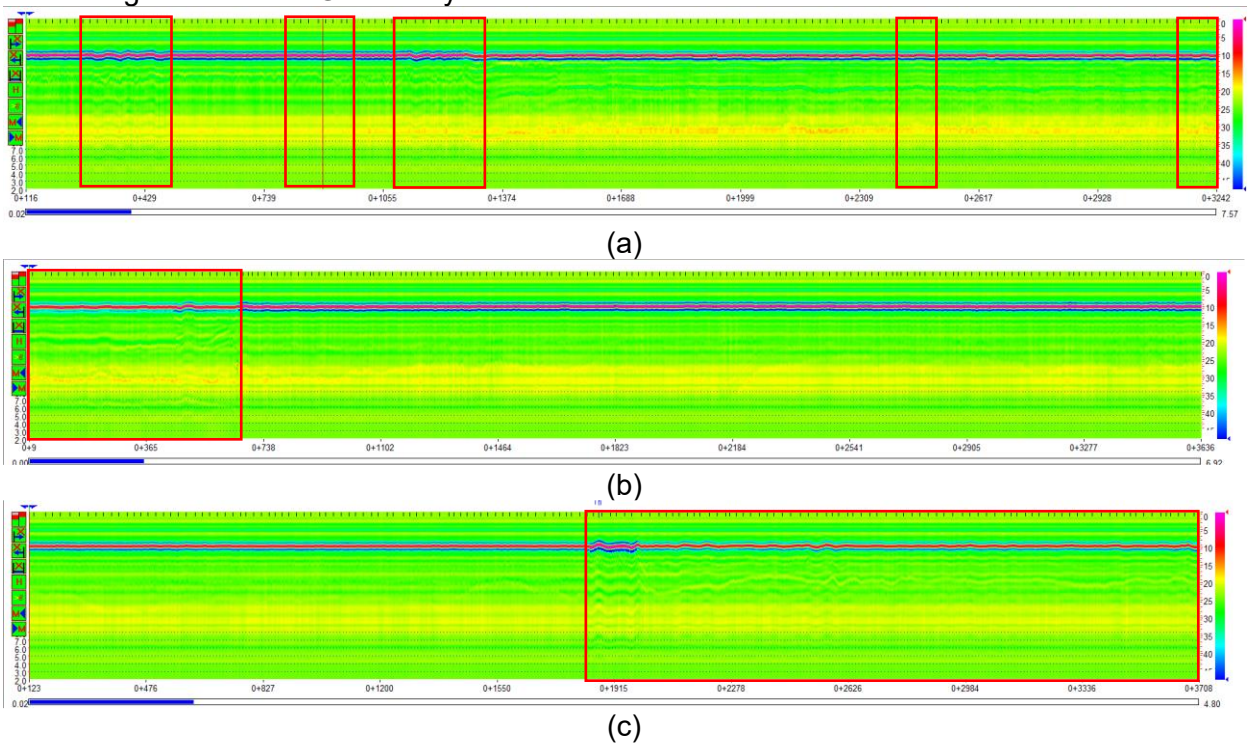

(a)

(b)

(c)

Figure 33 GPR Images of I-35 experimental sites: (a) Section 1 (fair), (b) Section 2 (good) and (c) Section 3 (poor)

4.7.2 GPR Images of I-40 Experimental Sites:

Figures 34(a), 34(b) and 34(c) present the GPR images of I-40 Section 1, Section 2 and Section 3, respectively. The I-40 experimental sites were found to be mostly flexible pavements of approximately 10-inches of thickness. From Figure 34(a), I-40 Section 1 was found to show significant distresses within asphalt and subsurface layers. The results match with Pave3D 8k findings as %cracking on the wheel and non-wheel paths for those areas were found to be significantly higher than other areas. Similarly, I-40 Section 3 was found to exhibit higher surface and subsurface distresses. It was assumed that these high distresses contributed to the overall rating of the pavement sections as I-40 Section 1 and Section 3 were rated as poor and fair conditioned from TSD analysis. Some distresses on the subsurface were observed over the I-40 Section 2 (Figure 34(b)) which was categorized as good conditioned from TSD analysis. The FWD analysis showed very high elastic modulus for the surface layer which may have contributed to the rating of this experimental site.

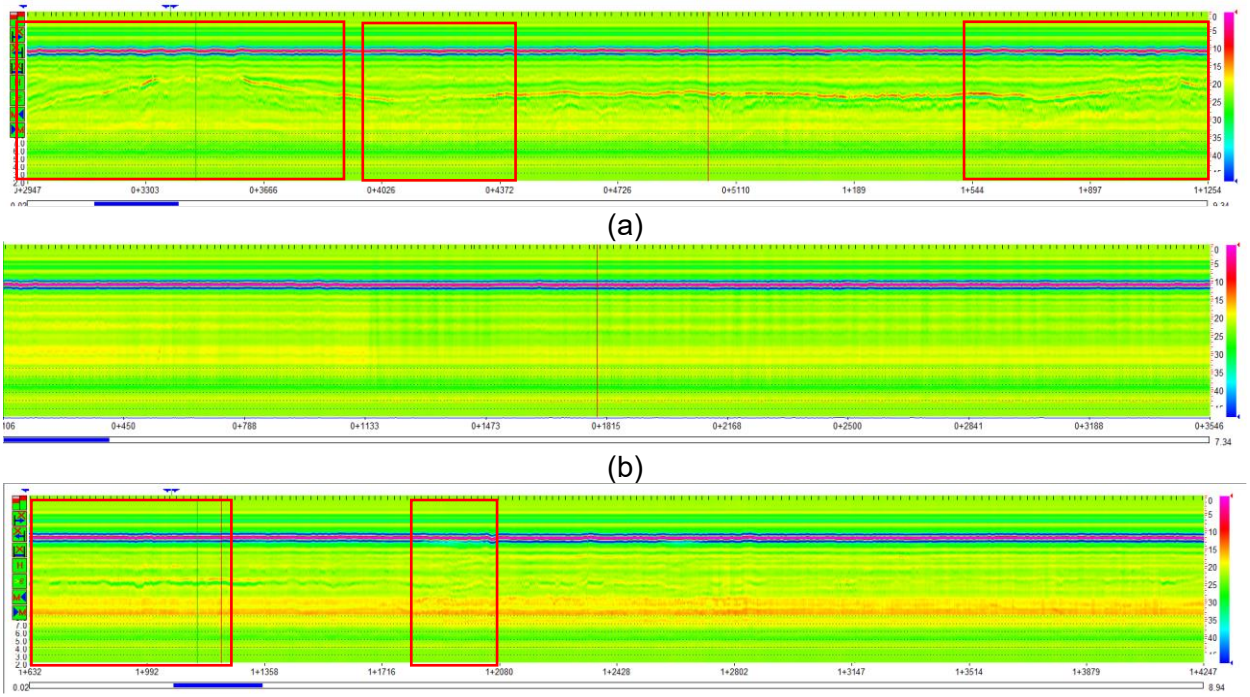

(a)

(b)

(c)

Figure 34 GPR Images of I-40 experimental sites: (a) Section 1 (poor), (b) Section 2 (good) and (c) Section 3 (fair)

4.8 Correlation Between Pavement Condition Parameters

In this study, an attempt was made to determine the correlations between different network-level parameters obtained from the TSD data and in-house technologies. For this purpose, a test matrix was formed using the TSD basin parameters, FFWD Layer Moduli (E1), FFWD W1 and W6 deflection data, Pave 3D 8K rutting (RD), wheel path cracking (CWP), non-wheel path cracking (CNWP) and MPD from the initially categorized pavement sections of I-35 and I-40. A total of 52 advanced machine learning models, including, Random Forest Regression, Gradient Boosting Regression, KNeighbors Regression, Decision Tree and Linear Regressions were used for evaluating the relationships among different parameters. From previous discussions, it was found that the structural conditions of I-35 and I-40 are significantly different. Therefore, in order to reduce variability, the regression analyses between different parameters for I-35 and I-40 experimental sites were conducted separately. The Coefficient of Correlation (R^2) between independent and dependent variables were used to determine the goodness of fit of the relationships using the following thresholds:

$R^2 < 0.3$: Weak fit
$0.3 \leq R^2 < 0.60$: Moderate fit
$0.60 \leq R^2 < 0.9$: Strong fit
$R^2 \geq 0.9$: Very strong fit (or excellent fit)

4.8.1 Comparison of FFWD and TSD parameters

4.8.1.1 I-35 Experimental Sites

A summary of the regression analyses of the FFWD normalized (9-kip) W1 deflection with TSD basin parameters for I-35 experimental sites using above models is presented in Table 8. From Table 8, it was observed that the SCI300, BCI, D1500 and AUPP parameters from TSD have strong correlations with the FFWD W1 deflection ($R^2 \geq 0.67$). This was found to be true for all models considered in these analyses. Examples of the variations of SCI300 and AUPP from TSD with FFWD W1 deflection are presented in Figures 35(a) and 35(b), respectively. A similar analysis was also performed using the FFWD E1 and W6 deflection with TSD parameters. Table 9 shows the correlation analyses among FFWD E1 and TSD basin parameters for I-35 experimental sites. Strong relationships were observed between FFWD E1 and TSD basin parameters. However, a poor relationship was observed between the FFWD W6 deflections and TSD parameters (Appendix A). Details of the regression analyses can be found in Appendix A.

Table 8 Regression Analysis for FFWD W1 and TSD Basin Parameters for I-35

Parameter	Max R^2	Fitting Model
SCI300	0.81	K-Neighbors Regressor
AUPP	0.78	K-Neighbors Regressor
D1500 and SCI300	0.79	K-Neighbors Regressor
D1500 and BCI	0.67	Random Forest Regressor
D1500 and AUPP	0.80	K-Neighbors Regressor
SCI300 and BCI	0.73	Random Forest Regressor
SCI300 and AUPP	0.76	K-Neighbors Regressor
BCI, SCI300 and AUPP	0.80	K-Neighbors Regressor
BCI, SCI300, D1500 and AUPP	0.76	K-Neighbors Regressor

Table 9 Regression Analysis for FFWD E1 and TSD Basin Parameters for I-35

Parameter	Max R^2	Fitting Model
SCI300	0.75	Gradient Boosting Regressor
AUPP	0.65	Random Forest Regressor
D1500 and SCI300	0.75	Random Forest Regressor
D1500 and BCI	0.72	Random Forest Regressor
BCI and AUPP	0.80	K-Neighbors Regressor
SCI300 and BCI	0.80	Random Forest Regressor
SCI300 and AUPP	0.77	Random Forest Regressor
D1500, SCI300 and BCI	0.80	Gradient Boosting Regressor
BCI, SCI300, D1500 and AUPP	0.79	Gradient Boosting Regressor

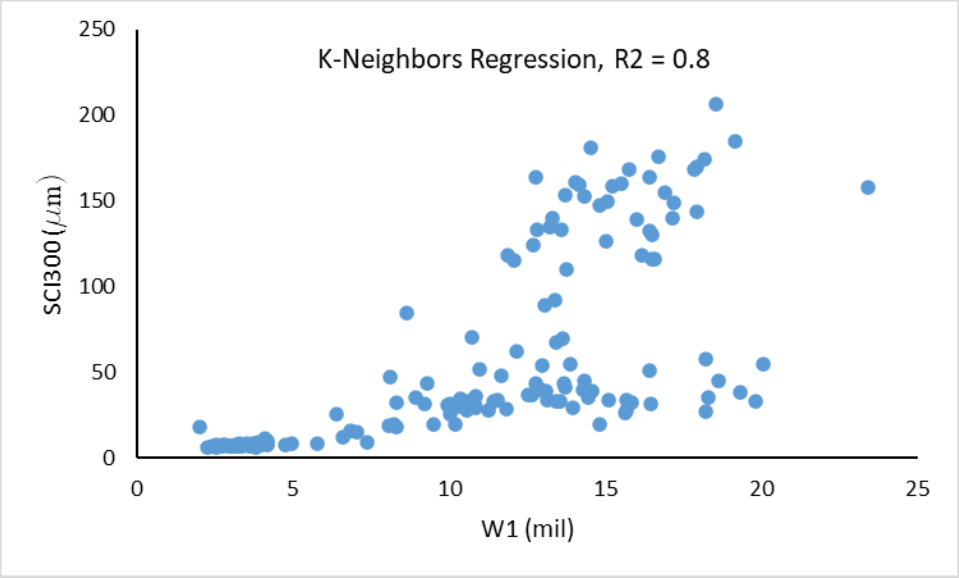

(a)

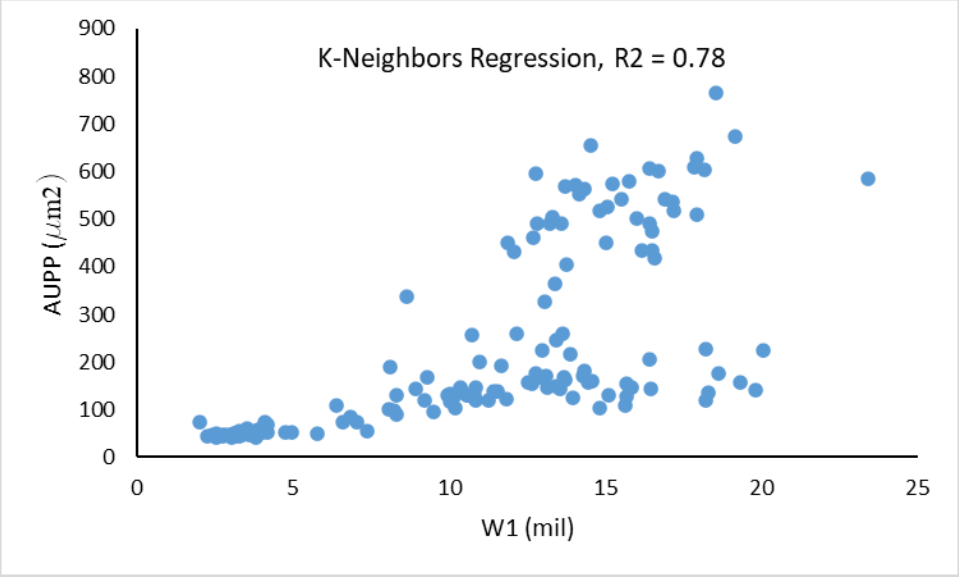

(b)

Figure 35 Variation of TSD basin parameters with FFWD W1 deflection for I-35: (a) SCI300; and (b) AUPP

4.8.1.2 I-40 Experimental Sites

A similar analysis was also conducted for I-40 experimental sites. Summaries of correlation analyses between FFWD W1 and E1 with TSD parameters are presented in Tables 10 and 11, respectively. The above-mentioned TSD parameters were found to show a moderate correlation with FFWD W1 deflection when considered individually. However, the combined effect of BCI, SCI300 and AUPP were found to show a strong relationship with the W1 deflection as evident from Table 10. From Table 11, the SCI300, BCI, D1500 and AUPP were found to show strong relationships with FFWD E1. Overall, the results suggest that strong correlations between FFWD W1 and E1 with TSD basin parameters allow them to be used interchangeably for assessing pavement structural conditions and ranking at the network-level.

Table 10 Regression Analysis for FFWD W1 and TSD Basin Parameters for I-40

Parameter	Max R^2	Fitting Model
SCI300	0.62	K-Neighbors Regressor
AUPP	0.65	K-Neighbors Regressor
BCI and SCI300	0.63	Gradient Boosting Regressor
SCI300 and AUPP	0.65	K-Neighbors Regressor
BCI, SCI300 and AUPP	0.68	Gradient Boosting Regressor

Table 11 Regression Analysis for FFWD E1 and TSD Basin Parameters for I-40

Parameter	Max R^2	Fitting Model
SCI300	0.83	Decision Tree Regressor
AUPP	0.86	K-Neighbors Regressor
D1500 and SCI300	0.89	Gradient Boosting Regressor
D1500 and AUPP	0.87	K-Neighbors Regressor
BCI and AUPP	0.80	K-Neighbors Regressor
SCI300 and BCI	0.91	Gradient Boosting Regressor
SCI300 and AUPP	0.87	Random Forest Regressor
D1500, SCI300 and BCI	0.93	Gradient Boosting Regressor
BCI, SCI300, D1500 and AUPP	0.88	K-Neighbors Regressor

4.8.2 Comparison of FFWD and Pave3D 8k parameters

4.8.2.1 I-35 Experimental Sites

Table 12 shows a summary of the regression analyses of FFWD normalized W1 deflection and Pave 3D 8K surface parameters for I-35 experimental sites. Table 12 only shows the results of selected models. The details of the results can be found in Appendix A. A moderate correlation was observed between the FFWD normalized W1 deflection with Pave3D 8K RD, MPD, %CWP and %CNWP parameters with a maximum R^2 value of 0.60. Similar moderate fits were observed between FFWD E1 and Pave3D 8K surface parameters for I-35 with a maximum R^2 value of 0.50 (Table 13).

Table 12 Regression Analysis FFWD W1 and Pave3D 8K Parameters for I-35

Parameter	Max R^2	Fitting Model
MPD, %CNWP	0.58	K-Neighbors Regressor
%CWP, %CNWP	0.57	Gradient Boosting Regressor
RD, %CWP, %CNWP	0.60	Random Forest Regressor
MPD, %CWP, %CNWP	0.54	K-Neighbors Regressor
RD, MPD, %CWP, %CNWP	0.60	K-Neighbors Regressor

Table 13 Regression Analysis for FFWD E1 and Pave3D 8K Surface Parameters for I-35

Parameter	Max R^2	Fitting Model
RD and MPD	0.5	Random Forest Regressor
MPD and %CWP	0.5	K-Neighbors Regressor
RD and %CWP	0.5	Random Forest Regressor
RD, %CWP and %CNWP	0.5	K-Neighbors Regressor
MPD, %CWP and %CNWP	0.5	K-Neighbors Regressor

4.8.2.2 I-40 Experimental Sites

Tables 14 and 15 show the summaries of the regression analyses of the FFWD normalized W1 deflection and E1 modulus with Pave 3D 8K surface parameters for I-40 experimental sites, respectively. From Table 14, the correlations between Pave3D 8K parameters and FFWD normalized W1 deflection were found to be moderate. However, FFWD E1 and Pave3D 8K surface parameters for I-40 experimental sites exhibited strong correlations with a maximum R^2 value of 0.93 for MPD. The results indicate that the in-house Pave3D 8K technology show moderate to strong correlation with FFWD parameters and can be used to classify the pavement network into different categories.

Table 14 Regression Analysis FFWD W1 and Pave3D 8K Parameters for I-40

Parameter	Max R^2	Fitting Model
%CWP and %CNWP	0.55	K-Neighbors Regressor
RD, MPD and %CWP	0.65	Random Forest Regressor
RD, MPD, %CWP and %CNWP	0.51	K-Neighbors Regressor

Table 15 Regression Analysis for FFWD E1 and Pave3D 8K Surface Parameters for I-40

Parameter	Max R^2	Fitting Model
MPD	0.93	Random Forest Regressor
RD and MPD	0.90	Random Forest Regressor
MPD and %CWP	0.82	Random Forest Regressor
MPD and %CNWP	0.85	Random Forest Regressor
%CWP and %CNWP	0.76	Decision Tree Regressor
RD, MPD and %CWP	0.89	Random Forest Regressor
RD, MPD and %CNWP	0.90	K-Neighbors Regressor
RD, %CWP and %CNWP	0.64	K-Neighbors Regressor
MPD, %CWP and %CNWP	0.88	K-Neighbors Regressor
RD, MPD, %CWP and %CNWP	0.86	Random Forest Regressor

4.8.3 Comparison of Pave3D 8k and TSD parameters

In this study, regression analyses were performed between Pave3D 8K and TSD basin parameters to understand their relationships. The details of the analyses considering all TSD and Pave3D 8K parameters are presented in Appendix A. The correlations between Pave3D 8K %CWP and %CNWP with TSD basin parameters for I-35 experimental sites are presented in Tables 16 and 17, respectively. It was observed that the %CWP and %CNWP from Pave3D 8K

showed moderate fit with TSD parameters with a maximum R^2 value of 0.70. The correlations between %CWP and TSD basin parameters for I-40 sites were weaker than I-35 sites, as seen from Table 18. The RD and MPD from Pave3D 8K did not show any meaningful correlations with TSD basin parameters. Therefore, RD and MPD from Pave3D 8K were excluded from further analyses.

Table 16 Regression Analysis for Pave 3D 8K %CWP and TSD Basin Parameters for I-35

Parameters	Max R^2	Fitting Model
AUPP	0.62	K-Neighbors Regressor
D1500, SCI300	0.70	K-Neighbors Regressor
D1500, BCI	0.60	K-Neighbors Regressor
D1500, AUPP	0.61	K-Neighbors Regressor
SCI300, BCI	0.61	K-Neighbors Regressor
SCI300, AUPP	0.66	K-Neighbors Regressor
BCI, AUPP	0.67	K-Neighbors Regressor
D1500, BCI, AUPP	0.64	K-Neighbors Regressor
SCI300, BCI, AUPP	0.61	K-Neighbors Regressor

Table 17 Regression Analysis for Pave 3D 8K %CNWP and TSD Basin Parameters for I-35

Parameters	Max R2	Fitting Model
SCI300	0.61	K-Neighbors Regressor
AUPP	0.62	Gradient Boosting Regressor
D1500, SCI300	0.62	Random Forest Regressor
D1500, BCI	0.67	Random Forest Regressor
D1500, AUPP	0.62	Gradient Boosting Regressor
SCI300, BCI	0.62	K-Neighbors Regressor
BCI, AUPP	0.61	Random Forest Regressor
D1500, SCI300, BCI	0.66	Gradient Boosting Regressor
D1500, SCI300, AUPP	0.62	K-Neighbors Regressor
D1500, BCI, AUPP	0.65	Random Forest Regressor
SCI300, BCI, AUPP	0.63	K-Neighbors Regressor
D1500, SCI300, BCI, AUPP	0.65	Gradient Boosting Regressor

Table 18 Regression Analysis for Pave 3D 8K %CWP and TSD Basin Parameters for I-40

Parameter	Max R2	Fitting Model
D1500, SCI300	0.51	K-Neighbors Regressor
D1500, AUPP	0.54	Gradient Boosting Regressor
D1500, SCI300, BCI	0.53	Gradient Boosting Regressor
D1500, SCI300, AUPP	0.52	K-Neighbors Regressor
D1500, SCI300, BCI, AUPP	0.51	Random Forest Regressor

4.8.4 Determining Thresholds for Pavement Condition Rating

The regression analysis conducted in the previous sections was used to identify parameters that can serve as indicators of pavement performance. Since the FWD test has been widely used by the transportation community for several decades, the parameters that showed strong correlations with FFWD E1 and W1-normalized deflection were selected as reliable indicators of pavement condition. Accordingly, in this study, SCI300 from the TSD data, along with %CWP and %CNWP from the Pave3D-8K system, were chosen as the primary parameters for assessing pavement conditions.

For this purpose, Annual Average Daily Traffic (AADT) data for the experimental sites were obtained from the ODOT database. Based on the AADT values, the Equivalent Single Axle Load (ESAL) was calculated for 1-year, 2-year, and 5-year periods. Using the FFWD E1 data and the SCI300 values from the TSD, the remaining fatigue life (Nf) of the asphalt layers was estimated using Equation 7. Pavement sections were classified as follows:

- **Good:** Nf > 5-year ESAL
- **Fair:** Nf between 2-year and 5-year ESAL
- **Poor:** Nf < 2-year ESAL

A gradient boosting machine-learning model was then developed and executed to evaluate the relationship between SCI300 and Nf. Figure 36 presents the relationship between Nf and SCI300 for the I-35 and I-40 pavement sections. These models were subsequently used to determine threshold values for SCI300. The were further calculated and suggested as the threshold values for these parameters. Following the regression analyses, threshold limits for the W1, %CWP and %CNWP were calculated by taking average of these parameters from the categorized sections (which were categorized as good, fair and poor based on the SCI300) for I-35 and I-40 were established and are summarized in Tables 19 and 20, respectively.

The initial network-level pavement ratings for I-35 and I-40 based on the TSD data were consistent with the results obtained from the FFWD and Pave3D-8K systems. A similar trend was observed across all three technologies for all evaluated sections. Therefore, these threshold limits can be used to classify pavement networks into good, fair, and poor categories to support the prioritization of pavement maintenance activities.

$$N_f = C \times 0.00432 \left(\frac{1}{\varepsilon_t}\right)^{3.291} \left(\frac{1}{E}\right)^{0.854} \quad (7)$$

Where,

C, a' and b'= constants,

ε_t = tensile strength at the bottom of the AC layer = $\varepsilon = a'(SCI\,300)^{b'}$

E = modulus of elasticity of AC layer

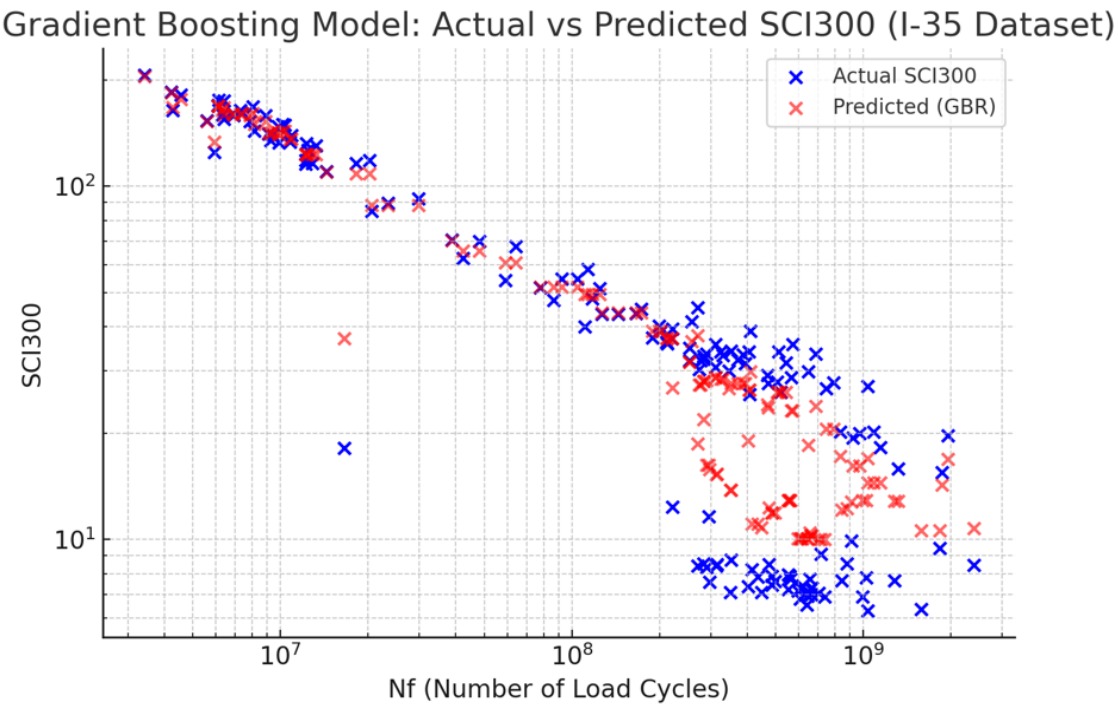

(a)

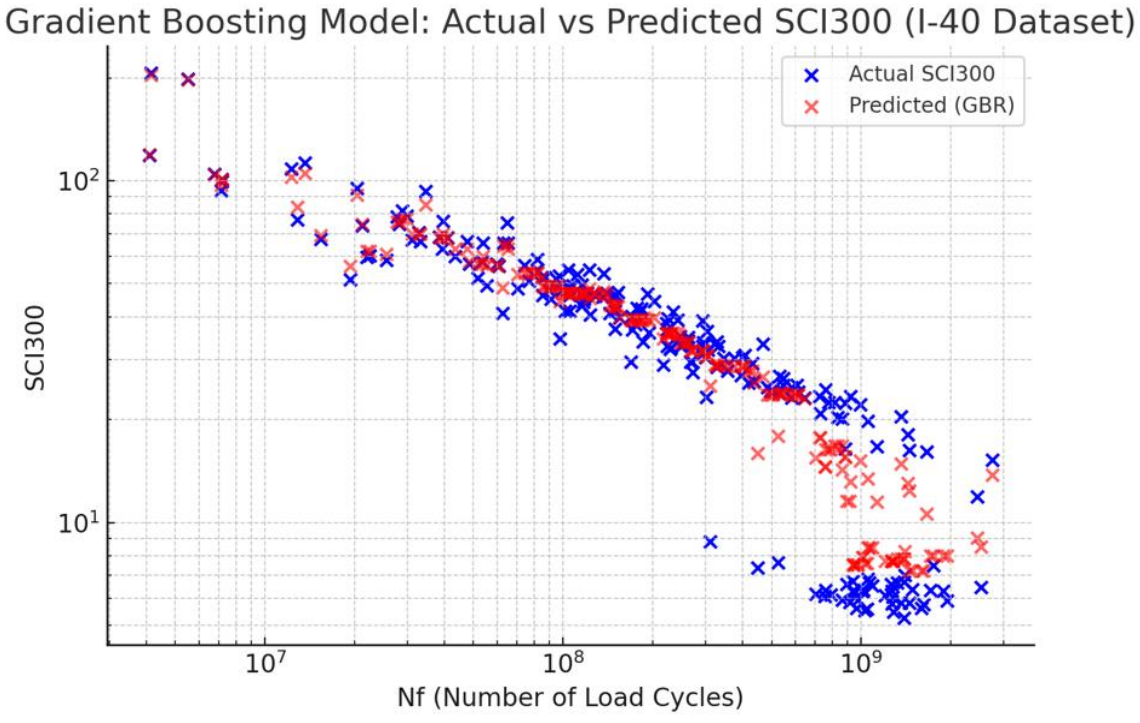

(b)

Figure 36 Relationship of SCI300 and Nf: (a) I-35; and (b) I-40

Table 19 Refined Pavement Condition Thresholds for I-35 Pavement

Category	SCI300, mm	Pave3D 8K %CWP	Pave3D 8K %CNWP	FFWD W1 (μm)
Good	**<140**	**<1.6**	**<1.7**	**<167**
Fair	**140-215**	**1.6-1.7**	**1.7-2.2**	**167-510**
Poor	**>215**	**>1.7**	**>2.2**	**>510**

Table 20 Refined Pavement Condition Thresholds for I-40 Pavement

Category	SCI300 (mm)	Pave3D 8K %CWP	Pave3D 8K %CNWP	FFWD W1 (μm)
Good	<140	<0.35	<2.6	<115
Fair	140-200	0.35-1.5	2.6-2.7	115-337
Poor	>200	>1.5	>2.7	>337

Chapter 5. Conclusions and Recommendations

The focus of this collaborative project was to evaluate tools for rapidly and cost-effectively assessing network-level pavement conditions for Oklahoma. As part of ODOT's engagement in a pooled fund study (TPF-5 (385)), pavement conditions data from I-35 and I-40 in Oklahoma were collected recently using a TSD. This study focused on analyzing the collected TSD data for network-level assessment or rating of the associated pavement. A complementary objective was to collect data from the same pavements using in-house technologies, namely Pave3D 8K available at OSU and an air-coupled Ground Penetrating Radar (GPR) and Fast Falling weight Deflectometer (FFWD) and compare with TSD data. In addition, this study focused on investigating the correlation among TSD deflection basin parameters, FFWD structural capacity parameters, and Pave3D 8K parameters using advanced machine learning models. The following conclusions and recommendations were drawn from this study:

- TSD provided continuous, high-speed deflection data, enabling network-level structural evaluations without disrupting traffic. TSD deflection basin parameters, namely SCI300, BCI and D1500 with threshold limits from current literature were used for categorizing pavement conditions at network-level. Care should be taken in analyzing the TSD data as it requires significant time and experience. As TSD produces massive amounts of data, care should be taken in cleaning the data before analysis.
- From TSD data analysis, slightly different pavement rankings were observed based on different TSD basin parameters. Based on SCI300 indices, it was observed that most of the I-35 sections were categorized as good conditioned. However, many of the I-40 EB and I-40 WB sections fell under fair to poor categories based on SCI300. It was observed that almost all of I-35 SB and I-40 EB have BCI values less than 76.02 μm, representing good conditions of the pavements. Some sections of I-40 WB were found to exhibit fair conditions from BCI index. Based on D1500, it was observed that most of the I-35 SB, I-40 EB and I-40 WB sections fell under good to fair conditions, indicating strong subgrade layers.
- Pavement surface conditions of the experimental sites identified using TSD analysis were assessed using the Pave3D 8K. The pavement categorization of I-35 experimental sites using rut depths was found to be same as TSD categorization. However, the I-40 experimental sites showed slightly different categorization between TSD and rut depths from Pave3D 8K. For both I-35 and I-40 sites, the MPD results did not match the TSD results. The %CWP and %CWNP from Pave3D 8K were in agreement with the TSD results based on I-35 sites. However, The %CWP and %CWNP results show that the pavement conditions across all I-40 experimental sites are nearly identical, making it challenging to differentiate between them. Therefore, an integrated categorization that considers both structural and functional aspects is essential for the effective management of pavement infrastructure systems.
- Field coring was found to provide insight into pavement categorization using TSD. The I-35 experimental site (Section 2) was found to have a composite structure (concrete over asphalt) and was ranked as good conditioned. Whereas the other two experimental sites consisted of only asphalt materials and were ranked as good and fair conditioned. Also, the pavement categorization using rut depths from Face Dipstick matched with the ranking obtained from the TSD analysis.
- The FFWD results indicated that the pavement rankings obtained from W1 deflection and E1 modulus are similar to TSD classifications for I-35 experimental sites. The I-40 good experimental site was ranked as good from FFWD W1 deflection and E1 modulus.

However, the ranking was the poor- and fair-conditioned experimental sites did not match with TSD ranking.

- The GPR images were found to provide information related to layer thicknesses and subsurface anomalies with potential issues that may not manifest as surface damage. For both I-35 and I-40 experimental sites, the ranking from TSD analysis was found to be in agreement with GPR analysis.
- An attempt was made to determine the correlations between different network-level parameters obtained from the TSD data and in-house technologies using advanced machine learning models. The results suggest that strong correlations between FFWD W1 and E1 with TSD basin parameters allow them to be used interchangeably for assessing pavement structural conditions and ranking at the network-level. It was observed that the %CWP and %CNWP from Pave3D 8K showed moderate fit with SCI300, BCI and AUPP, whereas the RD and MPD did not show any meaningful correlations with TSD basin parameters.
- Based on the collected data and regression analyses, the thresholds for TSD, FFWD and Pave3D 8K parameters were set in such a way that at least 75th percentile data of a particular section fell under that category. The thresholds can be used for classifying the pavement network into good, fair and poor categories for prioritizing pavement maintenance works.

Chapter 6. Implementation of Project Outputs

This study provided valuable insights on the use of different tools and technologies for DOT's pavement condition evaluation and management system. Using advanced technologies, like TSD, Pave3D 8K technology, and other instruments, this study aimed to change how DOTs evaluate and manage infrastructure health on a network-level. This study was focused on analyzing the collected TSD data from I-35 and I-40 pavement sections in Oklahoma for network-level assessment or rating. The network-level pavement ratings obtained from TSD parameters were compared with pavement ratings obtained from FFWD, Pave3D 8K, GPR and other field assessments. Advanced machine learning models were used to determine the correlations between different network-level parameters obtained from different technologies. Based on the collected data and regression analyses, the thresholds for TSD, FFWD and Pave3D 8K parameters were determined to rank pavements into poor, fair and good categories. These thresholds can be used by ODOT and other DOTs' for classifying the pavement network for prioritizing pavement maintenance works.

The findings are expected to bring about positive changes and help meet USDOT strategic goal to reduce backlog of pavement repairs to enhance economic strength. Consideration of different technologies and parameters will allow for improved pavement health assessments, more accurate life-cycle cost analyses, and targeted maintenance strategies, ultimately leading to more resilient, cost-effective and data-driven pavement management systems. Also, the adoption of this rating system will bridge the gap between network-level monitoring and project-level diagnostics. As a result, it empowers transportation agencies to prioritize resources effectively, mitigate risks proactively, and extend the service life of pavement assets.

Chapter 7. Technology Transfer and Community Engagement and Participation (CEP) Activities

The research team has worked towards disseminating the findings of this study to the stakeholders and engineering community through oral and poster presentations. Also, the team is working on preparing a journal manuscript from this study. In addition, the team is planning to conduct a technology transfer workshop to train to disseminate the findings and train DOTs on the use of TSD data and other technologies. The research team worked closely with the Oklahoma DOT, specifically Mr. Angel Gonzales for the successful completion of this project. Mr. Gonzales helped to access TSD data and was involved in the progress meetings to provide feedback. ODOT District 4 helped coordinate the collection of FFWD and other field data. The findings are expected to be implemented by ODOT as well as DOTs in Region 6 for pavement management and rehabilitation.

Chapter 8. Invention Disclosures and Patents, Publications, Presentations, Reports, Project Website, and Social Media Listings

The research team has worked towards disseminating the findings of this study to the stakeholders and engineering community. Till now, the team has made two oral presentations, and one poster presentation based on the findings of this study. Also, the team is working on preparing a journal manuscript from this study. The list of the presentation and publication is as follows:

- Ghos, S., Mendez Larrain, M., Ali, S. A., Hobson, K., Zaman, M., 2024 Oklahoma Transportation Research Day (OTRD), "Novel Tools for Rapid Assessment of Pavement Conditions," Oklahoma Department of Transportation, Oklahoma City, OK. (October 15, 2024). Poster, Conference.
- Ghos, S., Mendez Larrain, M., Ali, S. A., Hobson, K., Zaman, M., 59th Annual Paving and Transportation Conference, "Novel Tools for Rapid Assessment of Pavement Conditions," University of New Mexico, Albuquerque, NM. (January 3, 2024). Oral Presentation, Conference.
- Ghos, S., Ali, S. A., Zaman, M., Mendez Larrain, M., Hobson, K., (2025), "Development of Network-Level Thresholds for Rapid Assessment of Pavement Conditions in Oklahoma," Under Preparation.

References

- Bryce, J.M., Flintsch, G.W., Katicha, S.W. and Diefenderfer, B.K., 2013. Developing a network-level structural capacity index for structural evaluation of pavements. Virginia Center for Transportation Innovation and Research.
- Chang, C., Saenz, D., Nazarian, S., Abdallah, I. N., Wimsatt, A., Freeman, T., & Fernando, E. G. (2014). *TXDOT guidelines to assign PMIS treatment levels* (No. 0-6673-P1). Texas. Dept. of Transportation. Research and Technology Implementation Office.
- Tennessee DOT, 2025. Pavement Management. Pavement Management. Tennessee DOT, website last accesses on December 2024.
- Shrestha, S., 2017. Development of structural condition thresholds for TSD measurements (Doctoral dissertation, Virginia Tech).
- Zihan, Z.U.A., 2019. Evaluation of Traffic Speed Deflectometer for Pavement Structural Evaluation in Louisiana. Louisiana State University and Agricultural & Mechanical College.
- Zhang, Z., Manuel, L., Damnjanovic, I. and Li, Z., 2003. Development of a new methodology for characterizing pavement structural condition for network-level applications. Texas Dept. of Transportation, Austin, TX.
- Rada, G. R., Nazarian, S., Visintine, B. A., Siddharthan, R. V., & Thyagarajan, S. (2016). Pavement structural evaluation at the network level (No. FHWA-HRT-15-074). United States. Federal Highway Administration. Office of Infrastructure Research and Development.
- Rohde, G. T. (1994). Determining pavement structural number from FWD testing. Transportation Research Record, (1448).
- Peraka, N. S. P., & Biligiri, K. P. (2020). Pavement asset management systems and technologies: A review. Automation in Construction, 119, 103336.
- Snyder, "Snyder & Associates," 2022. [Online]. Available: https://www.snyder-associates.com/optimize-roadway-network-pavement-management-system/.
- G. Flintsch and K. McGhee, "Synthesis: Managing the quality of pavement data collection," National Cooperative Highway, 2009.
- G. Flintsch, B. Ferne, B. Diefenderfer, S. Katicha, J. Bryce and S. Nell, "Evaluation of Traffic-Speed Deflectometers," Transportation Research Record, 2304, 37 - 46., 2012.
- S. Katicha, S. Shrestha, G. Flintsch and B. Diefendender, "Network Level Pavement Structural Testing with the Traffic Speed Deflectometer," Virginia Department of Transportation (VDOT), 2020.
- C. W. R. Triplow, "An Evaluation of Traffic Speed Deflectometer for Main Roads Western Australia," Australian Road Research Board, 2017.
- L. GeoSolve, "Traffic Speed Deflectometer: The Application of TSD Data in New Zealand for Asset Management and Design," New Zealand Trasnportation Agency, 2016.
- G. Rada and S. Nazarian, "The State-of-the-Technology of Moving Pavement Deflection Testing," FHWA, 2011.
- H. Schnoor and E. Horak, "Possible Method of Determining Structural Number for Flexible Pavements with the Falling Weight Deflectometer," in 31st Southern African Transport Conference (SATC 2012) , Pretoria, South Africa, 2012.

- M. Elseifi and X. Zihan, "Assessment of the Traffic Speed Deflectometer in Louisiana for Pavement Structural Evaluation," Louisiana Transportation Research Center, 2018.
- ARRB, "AN EVALUATION OF THE TRAFFIC SPEED DEFLECTOMETER FOR MAIN ROADS WESTERN AUSTRALIA," ARRB, 2017.
- H. Huang, Pavement Analysys and Design, 2nd Edition ed., Pearson, 2004.
- S. Noureldin, K. Zhu, D. Harris and S. Li, "Non-Destructive Estimation of Pavement Thickness, Structural Number, and Subgrade Resilience Along INDOT Highways," Indiana DOT, 2005.
- M. Nasimifar, S. Thyagarajan, S. Chaudhari and N. Sivaneswaran, "Pavement Structural Capacity from Traffic Speed Deflectometer for Network Level Pavement Management System Application," Transportation Research Record, 2673(2), 456-465, 2019.
- Schnoor, H., & Horak, E. (2012). Possible method of determining structural number for flexible pavements with the falling weight deflectometer. SATC 2012.

Appendix A: Results of Regression Analysis

Table A.1 Summary of Regression Analysis for FFWD E1 to TSD Deflection Parameters

Model	Features	Accuracy (%)	MSE	R^2
LinearRegression	D1500	-4.1	3602669.4	0.0
GradientBoostingRegressor	D1500	-16.2	4020299.8	-0.2
DecisionTreeRegressor	D1500	-52.8	5286723.2	-0.5
RandomForestRegressor	D1500	-22.6	4240674.6	-0.2
KNeighborsRegressor	D1500	-4.4	3611403.3	0.0
HuberRegressor	D1500	-16.2	4018663.9	-0.2
LinearRegression	SCI300	20.9	2595918.5	0.2
GradientBoostingRegressor	SCI300	81.5	608172.9	0.8
DecisionTreeRegressor	SCI300	77.7	732406.8	0.8
RandomForestRegressor	SCI300	82.8	563485.6	0.8
KNeighborsRegressor	SCI300	85.2	484603.5	0.9
HuberRegressor	SCI300	16.2	2752271.7	0.2
LinearRegression	BCI	24.9	2354798.3	0.2
GradientBoostingRegressor	BCI	15.1	2659706.1	0.2
DecisionTreeRegressor	BCI	-2.6	3217100.4	0.0
RandomForestRegressor	BCI	22.1	2442994.6	0.2
KNeighborsRegressor	BCI	35.4	2025920.1	0.4
HuberRegressor	BCI	20.7	2484887.9	0.2
LinearRegression	AUPP	21.7	2568714.2	0.2
GradientBoostingRegressor	AUPP	61.6	1259035.2	0.6
DecisionTreeRegressor	AUPP	58.0	1379694.3	0.6
RandomForestRegressor	AUPP	66.9	1087784.2	0.7
KNeighborsRegressor	AUPP	81.6	604998.9	0.8
HuberRegressor	AUPP	17.1	2720044.3	0.2
LinearRegression	D1500 and SCI300	24.0	3000965.1	0.2
GradientBoostingRegressor	D1500 and SCI300	74.6	1001281.5	0.7
DecisionTreeRegressor	D1500 and SCI300	67.9	1267797.2	0.7
RandomForestRegressor	D1500 and SCI300	78.1	866227.5	0.8
KNeighborsRegressor	D1500 and SCI300	76.6	923410.8	0.8
HuberRegressor	D1500 and SCI300	16.9	3281275.9	0.2
LinearRegression	D1500 and BCI	22.6	2573803.3	0.2

Table A.1 Summary of Regression Analysis for FFWD E1 to TSD Deflection Parameters (cont.)

Model	Features	Accuracy (%)	MSE	R^2
GradientBoostingRegressor	D1500 and BCI	62.1	1260657.5	0.6
DecisionTreeRegressor	D1500 and BCI	53.8	1535051.4	0.5
RandomForestRegressor	D1500 and BCI	70.7	973881.8	0.7
KNeighborsRegressor	D1500 and BCI	54.9	1500346.6	0.5
HuberRegressor	D1500 and BCI	20.5	2642792.8	0.2
LinearRegression	D1500 and AUPP	22.9	3045331.4	0.2
GradientBoostingRegressor	D1500 and AUPP	61.6	1517210.7	0.6
DecisionTreeRegressor	D1500 and AUPP	61.6	1515744.1	0.6
RandomForestRegressor	D1500 and AUPP	69.4	1207296.5	0.7
KNeighborsRegressor	D1500 and AUPP	74.9	991030.1	0.7
HuberRegressor	D1500 and AUPP	15.8	3324190.5	0.2
LinearRegression	SCI300 and BCI	26.7	2649120.9	0.3
GradientBoostingRegressor	SCI300 and BCI	78.5	777679.9	0.8
DecisionTreeRegressor	SCI300 and BCI	74.5	921480.1	0.7
RandomForestRegressor	SCI300 and BCI	80.5	703582.7	0.8
KNeighborsRegressor	SCI300 and BCI	75.2	897412.4	0.8
HuberRegressor	SCI300 and BCI	22.4	2803411.0	0.2
LinearRegression	SCI300 and AUPP	21.8	2565428.6	0.2
GradientBoostingRegressor	SCI300 and AUPP	83.5	541959.2	0.8
DecisionTreeRegressor	SCI300 and AUPP	80.8	629280.8	0.8
RandomForestRegressor	SCI300 and AUPP	85.2	485938.7	0.9
KNeighborsRegressor	SCI300 and AUPP	82.0	591915.0	0.8
HuberRegressor	SCI300 and AUPP	17.4	2711443.5	0.2
LinearRegression	BCI and AUPP	26.2	2665996.7	0.3
GradientBoostingRegressor	BCI and AUPP	60.2	1437108.5	0.6
DecisionTreeRegressor	BCI and AUPP	58.9	1484014.6	0.6
RandomForestRegressor	BCI and AUPP	71.0	1048391.0	0.7
KNeighborsRegressor	BCI and AUPP	72.9	977248.2	0.7
HuberRegressor	BCI and AUPP	21.9	2821855.9	0.2
LinearRegression	D1500, SCI300 and BCI	29.8	2408466.6	0.3

Table A.1 Summary of Regression Analysis for FFWD E1 to TSD Deflection Parameters (cont.)

Model	Features	Accuracy (%)	MSE	R^2
GradientBoostingRegressor	D1500, SCI300 and BCI	80.7	660578.6	0.8
DecisionTreeRegressor	D1500, SCI300 and BCI	66.9	1136995.6	0.7
RandomForestRegressor	D1500, SCI300 and BCI	78.9	725295.8	0.8
KNeighborsRegressor	D1500, SCI300 and BCI	71.3	984963.1	0.7
HuberRegressor	D1500, SCI300 and BCI	26.7	2513329.9	0.3
LinearRegression	D1500, SCI300 and AUPP	24.3	2990586.1	0.2
GradientBoostingRegressor	D1500, SCI300 and AUPP	66.0	1344598.7	0.7
DecisionTreeRegressor	D1500, SCI300 and AUPP	58.7	1632684.6	0.6
RandomForestRegressor	D1500, SCI300 and AUPP	74.5	1007963.6	0.7
KNeighborsRegressor	D1500, SCI300 and AUPP	73.7	1038879.3	0.7
HuberRegressor	D1500, SCI300 and AUPP	17.1	3273906.8	0.2
LinearRegression	D1500, BCI, AUPP	28.5	2452997.5	0.3
GradientBoostingRegressor	D1500, BCI, AUPP	71.3	984305.1	0.7
DecisionTreeRegressor	D1500, BCI, AUPP	65.3	1190724.1	0.7
RandomForestRegressor	D1500, BCI, AUPP	71.9	962525.7	0.7
KNeighborsRegressor	D1500, BCI, AUPP	63.3	1258303.2	0.6
HuberRegressor	D1500, BCI, AUPP	25.4	2557827.8	0.3
LinearRegression	SCI300, BCI, AUPP	32.4	2441186.1	0.3
GradientBoostingRegressor	SCI300, BCI, AUPP	80.3	710656.7	0.8
DecisionTreeRegressor	SCI300, BCI, AUPP	80.0	721688.4	0.8
RandomForestRegressor	SCI300, BCI, AUPP	78.4	779883.7	0.8
KNeighborsRegressor	SCI300, BCI, AUPP	73.2	969567.7	0.7
HuberRegressor	SCI300, BCI, AUPP	28.9	2566686.8	0.3
LinearRegression	D1500, SCI300, BCI and AUPP	40.0	2059612.1	0.4
GradientBoostingRegressor	D1500, SCI300, BCI and AUPP	73.5	908377.6	0.7
DecisionTreeRegressor	D1500, SCI300, BCI and AUPP	64.1	1232561.1	0.6
RandomForestRegressor	D1500, SCI300, BCI and AUPP	76.8	795760.4	0.8
KNeighborsRegressor	D1500, SCI300, BCI and AUPP	68.1	1095585.9	0.7
HuberRegressor	D1500, SCI300, BCI and AUPP	35.8	2203563.1	0.4

Table A2. Summary of Regression Analysis for FFWD W1 to TSD Deflection Parameters

Model	Features	Accuracy (%)	MSE	R^2
LinearRegression	D1500	-0.3	24.5	0.0
GradientBoostingRegressor	D1500	-20.8	29.4	-0.2
DecisionTreeRegressor	D1500	-83.6	44.8	-0.8
RandomForestRegressor	D1500	-34.3	32.7	-0.3
KNeighborsRegressor	D1500	-10.5	26.9	-0.1
HuberRegressor	D1500	-0.2	24.4	0.0
LinearRegression	SCI300	51.2	10.3	0.5
GradientBoostingRegressor	SCI300	51.7	10.2	0.5
DecisionTreeRegressor	SCI300	31.4	14.5	0.3
RandomForestRegressor	SCI300	49.5	10.6	0.5
KNeighborsRegressor	SCI300	65.3	7.3	0.7
HuberRegressor	SCI300	51.9	10.1	0.5
LinearRegression	BCI	51.5	12.6	0.5
GradientBoostingRegressor	BCI	41.2	15.3	0.4
DecisionTreeRegressor	BCI	10.4	23.3	0.1
RandomForestRegressor	BCI	41.0	15.3	0.4
KNeighborsRegressor	BCI	59.1	10.6	0.6
HuberRegressor	BCI	51.0	12.7	0.5
LinearRegression	AUPP	52.2	10.1	0.5
GradientBoostingRegressor	AUPP	53.4	9.8	0.5
DecisionTreeRegressor	AUPP	24.2	16.0	0.2
RandomForestRegressor	AUPP	45.3	11.5	0.5
KNeighborsRegressor	AUPP	66.3	7.1	0.7
HuberRegressor	AUPP	52.8	9.9	0.5
LinearRegression	D1500 and SCI300	50.8	12.2	0.5
GradientBoostingRegressor	D1500 and SCI300	52.0	11.9	0.5
DecisionTreeRegressor	D1500 and SCI300	34.8	16.2	0.3
RandomForestRegressor	D1500 and SCI300	60.5	9.8	0.6
KNeighborsRegressor	D1500 and SCI300	67.8	8.0	0.7
HuberRegressor	D1500 and SCI300	52.0	11.9	0.5
LinearRegression	D1500 and BCI	54.7	9.8	0.5

Table A2. Summary of Regression Analysis for FFWD W1 to TSD Deflection Parameters (cont.)

Model	Features	Accuracy (%)	MSE	R^2
GradientBoostingRegressor	D1500 and BCI	64.3	7.7	0.6
DecisionTreeRegressor	D1500 and BCI	60.2	8.6	0.6
RandomForestRegressor	D1500 and BCI	71.5	6.2	0.7
KNeighborsRegressor	D1500 and BCI	69.8	6.6	0.7
HuberRegressor	D1500 and BCI	54.6	9.8	0.5
LinearRegression	D1500 and AUPP	53.5	11.6	0.5
GradientBoostingRegressor	D1500 and AUPP	59.4	10.1	0.6
DecisionTreeRegressor	D1500 and AUPP	50.9	12.2	0.5
RandomForestRegressor	D1500 and AUPP	66.4	8.4	0.7
KNeighborsRegressor	D1500 and AUPP	70.2	7.4	0.7
HuberRegressor	D1500 and AUPP	54.6	11.3	0.5
LinearRegression	SCI300 and BCI	55.7	9.9	0.6
GradientBoostingRegressor	SCI300 and BCI	63.4	8.2	0.6
DecisionTreeRegressor	SCI300 and BCI	59.2	9.1	0.6
RandomForestRegressor	SCI300 and BCI	66.1	7.6	0.7
KNeighborsRegressor	SCI300 and BCI	68.2	7.1	0.7
HuberRegressor	SCI300 and BCI	55.8	9.9	0.6
LinearRegression	SCI300 and AUPP	48.9	10.8	0.5
GradientBoostingRegressor	SCI300 and AUPP	55.5	9.4	0.6
DecisionTreeRegressor	SCI300 and AUPP	48.1	11.0	0.5
RandomForestRegressor	SCI300 and AUPP	57.9	8.9	0.6
KNeighborsRegressor	SCI300 and AUPP	67.1	6.9	0.7
HuberRegressor	SCI300 and AUPP	48.5	10.8	0.5
LinearRegression	BCI and AUPP	55.4	10.0	0.6
GradientBoostingRegressor	BCI and AUPP	58.9	9.2	0.6
DecisionTreeRegressor	BCI and AUPP	35.8	14.4	0.4
RandomForestRegressor	BCI and AUPP	64.3	8.0	0.6
KNeighborsRegressor	BCI and AUPP	68.4	7.1	0.7
HuberRegressor	BCI and AUPP	55.6	10.0	0.6
LinearRegression	D1500, SCI300 and BCI	54.7	9.5	0.5

Table A2. Summary of Regression Analysis for FFWD W1 to TSD Deflection Parameters (cont.)

Model	Features	Accuracy (%)	MSE	R^2
GradientBoostingRegressor	D1500, SCI300 and BCI	55.5	9.3	0.6
DecisionTreeRegressor	D1500, SCI300 and BCI	41.3	12.3	0.4
RandomForestRegressor	D1500, SCI300 and BCI	65.0	7.3	0.6
KNeighborsRegressor	D1500, SCI300 and BCI	74.5	5.3	0.7
HuberRegressor	D1500, SCI300 and BCI	54.6	9.5	0.5
LinearRegression	D1500, SCI300 and AUPP	54.3	11.3	0.5
GradientBoostingRegressor	D1500, SCI300 and AUPP	60.7	9.8	0.6
DecisionTreeRegressor	D1500, SCI300 and AUPP	52.5	11.8	0.5
RandomForestRegressor	D1500, SCI300 and AUPP	66.6	8.3	0.7
KNeighborsRegressor	D1500, SCI300 and AUPP	69.4	7.6	0.7
HuberRegressor	D1500, SCI300 and AUPP	55.1	11.2	0.6
LinearRegression	D1500, BCI and AUPP	54.1	9.6	0.5
GradientBoostingRegressor	D1500, BCI and AUPP	65.5	7.2	0.7
DecisionTreeRegressor	D1500, BCI and AUPP	35.2	13.6	0.4
RandomForestRegressor	D1500, BCI and AUPP	68.7	6.6	0.7
KNeighborsRegressor	D1500, BCI and AUPP	74.3	5.4	0.7
HuberRegressor	D1500, BCI and AUPP	54.1	9.6	0.5
LinearRegression	SCI300, BCI and AUPP	56.3	9.8	0.6
GradientBoostingRegressor	SCI300, BCI and AUPP	57.7	9.5	0.6
DecisionTreeRegressor	SCI300, BCI and AUPP	37.0	14.1	0.4
RandomForestRegressor	SCI300, BCI and AUPP	65.2	7.8	0.7
KNeighborsRegressor	SCI300, BCI and AUPP	71.3	6.4	0.7
HuberRegressor	SCI300, BCI and AUPP	56.4	9.8	0.6
LinearRegression	D1500, SCI300, BCI and AUPP	55.1	9.4	0.6
GradientBoostingRegressor	D1500, SCI300, BCI and AUPP	59.2	8.6	0.6
DecisionTreeRegressor	D1500, SCI300, BCI and AUPP	48.3	10.9	0.5
RandomForestRegressor	D1500, SCI300, BCI and AUPP	67.7	6.8	0.7
KNeighborsRegressor	D1500, SCI300, BCI and AUPP	76.2	5.0	0.8
HuberRegressor	D1500, SCI300, BCI and AUPP	55.1	9.4	0.6

Table A3. Summary of Regression Analysis for FFWD W6 to TSD Deflection Parameters

Model	Features	Accuracy (%)	MSE	R^2
LinearRegression	D1500	-2.9	0.3	0.0
GradientBoostingRegressor	D1500	-2.8	0.3	0.0
DecisionTreeRegressor	D1500	-38.0	0.3	-0.4
RandomForestRegressor	D1500	-8.9	0.3	-0.1
KNeighborsRegressor	D1500	14.0	0.2	0.1
HuberRegressor	D1500	-8.5	0.3	-0.1
LinearRegression	SCI300	-0.6	0.2	0.0
GradientBoostingRegressor	SCI300	-34.1	0.3	-0.3
DecisionTreeRegressor	SCI300	-114.2	0.5	-1.1
RandomForestRegressor	SCI300	-48.4	0.3	-0.5
KNeighborsRegressor	SCI300	15.6	0.2	0.2
HuberRegressor	SCI300	0.2	0.2	0.0
LinearRegression	BCI	10.0	0.2	0.1
GradientBoostingRegressor	BCI	-24.6	0.3	-0.2
DecisionTreeRegressor	BCI	-61.8	0.4	-0.6
RandomForestRegressor	BCI	-27.0	0.3	-0.3
KNeighborsRegressor	BCI	7.7	0.2	0.1
HuberRegressor	BCI	9.9	0.2	0.1
LinearRegression	AUPP	-2.1	0.2	0.0
GradientBoostingRegressor	AUPP	-12.7	0.2	-0.1
DecisionTreeRegressor	AUPP	-70.4	0.4	-0.7
RandomForestRegressor	AUPP	-16.9	0.3	-0.2
KNeighborsRegressor	AUPP	22.2	0.2	0.2
HuberRegressor	AUPP	-1.3	0.2	0.0
LinearRegression	D1500 and SCI300	11.6	0.1	0.1
GradientBoostingRegressor	D1500 and SCI300	-9.3	0.2	-0.1
DecisionTreeRegressor	D1500 and SCI300	-103.6	0.3	-1.0
RandomForestRegressor	D1500 and SCI300	12.4	0.1	0.1
KNeighborsRegressor	D1500 and SCI300	31.0	0.1	0.3
HuberRegressor	D1500 and SCI300	14.6	0.1	0.1
LinearRegression	D1500 and BCI	-17.3	0.2	-0.2

Table A3. Summary of Regression Analysis for FFWD W6 to TSD Deflection Parameters (cont.)

Model	Features	Accuracy (%)	MSE	R^2
GradientBoostingRegressor	D1500 and BCI	-10.3	0.2	-0.1
DecisionTreeRegressor	D1500 and BCI	-84.4	0.4	-0.8
RandomForestRegressor	D1500 and BCI	-27.1	0.3	-0.3
KNeighborsRegressor	D1500 and BCI	-11.2	0.2	-0.1
HuberRegressor	D1500 and BCI	-12.4	0.2	-0.1
LinearRegression	D1500 and AUPP	11.8	0.1	0.1
GradientBoostingRegressor	D1500 and AUPP	5.3	0.2	0.1
DecisionTreeRegressor	D1500 and AUPP	-14.7	0.2	-0.1
RandomForestRegressor	D1500 and AUPP	25.7	0.1	0.3
KNeighborsRegressor	D1500 and AUPP	35.9	0.1	0.4
HuberRegressor	D1500 and AUPP	14.8	0.1	0.1
LinearRegression	SCI300 and BCI	29.8	0.2	0.3
GradientBoostingRegressor	SCI300 and BCI	34.0	0.2	0.3
DecisionTreeRegressor	SCI300 and BCI	4.0	0.2	0.0
RandomForestRegressor	SCI300 and BCI	41.5	0.1	0.4
KNeighborsRegressor	SCI300 and BCI	46.7	0.1	0.5
HuberRegressor	SCI300 and BCI	28.7	0.2	0.3
LinearRegression	SCI300 and AUPP	32.6	0.1	0.3
GradientBoostingRegressor	SCI300 and AUPP	19.1	0.2	0.2
DecisionTreeRegressor	SCI300 and AUPP	-35.6	0.3	-0.4
RandomForestRegressor	SCI300 and AUPP	15.8	0.2	0.2
KNeighborsRegressor	SCI300 and AUPP	22.7	0.2	0.2
HuberRegressor	SCI300 and AUPP	32.7	0.1	0.3
LinearRegression	BCI and AUPP	29.6	0.2	0.3
GradientBoostingRegressor	BCI and AUPP	45.9	0.1	0.5
DecisionTreeRegressor	BCI and AUPP	-9.4	0.3	-0.1
RandomForestRegressor	BCI and AUPP	39.7	0.1	0.4
KNeighborsRegressor	BCI and AUPP	41.7	0.1	0.4
HuberRegressor	BCI and AUPP	28.5	0.2	0.3
LinearRegression	D1500, SCI300 and BCI	3.3	0.2	0.0

Table A3. Summary of Regression Analysis for FFWD W6 to TSD Deflection Parameters (cont.)

Model	Features	Accuracy (%)	MSE	R^2
GradientBoostingRegressor	D1500, SCI300 and BCI	9.5	0.2	0.1
DecisionTreeRegressor	D1500, SCI300 and BCI	-35.8	0.3	-0.4
RandomForestRegressor	D1500, SCI300 and BCI	21.3	0.2	0.2
KNeighborsRegressor	D1500, SCI300 and BCI	20.3	0.2	0.2
HuberRegressor	D1500, SCI300 and BCI	3.4	0.2	0.0
LinearRegression	D1500, SCI300 and AUPP	33.5	0.1	0.3
GradientBoostingRegressor	D1500, SCI300 and AUPP	14.1	0.1	0.1
DecisionTreeRegressor	D1500, SCI300 and AUPP	-32.9	0.2	-0.3
RandomForestRegressor	D1500, SCI300 and AUPP	37.0	0.1	0.4
KNeighborsRegressor	D1500, SCI300 and AUPP	34.0	0.1	0.3
HuberRegressor	D1500, SCI300 and AUPP	32.8	0.1	0.3
LinearRegression	D1500, BCI and AUPP	2.9	0.2	0.0
GradientBoostingRegressor	D1500, BCI and AUPP	14.4	0.2	0.1
DecisionTreeRegressor	D1500, BCI and AUPP	-21.4	0.3	-0.2
RandomForestRegressor	D1500, BCI and AUPP	22.5	0.2	0.2
KNeighborsRegressor	D1500, BCI and AUPP	15.3	0.2	0.2
HuberRegressor	D1500, BCI and AUPP	3.9	0.2	0.0
LinearRegression	SCI300, BCI and AUPP	30.1	0.2	0.3
GradientBoostingRegressor	SCI300, BCI and AUPP	37.6	0.1	0.4
DecisionTreeRegressor	SCI300, BCI and AUPP	-16.8	0.3	-0.2
RandomForestRegressor	SCI300, BCI and AUPP	41.3	0.1	0.4
KNeighborsRegressor	SCI300, BCI and AUPP	41.5	0.1	0.4
HuberRegressor	SCI300, BCI and AUPP	28.9	0.2	0.3
LinearRegression	D1500, SCI300, BCI and AUPP	3.5	0.2	0.0
GradientBoostingRegressor	D1500, SCI300, BCI and AUPP	4.3	0.2	0.0
DecisionTreeRegressor	D1500, SCI300, BCI and AUPP	-28.7	0.3	-0.3
RandomForestRegressor	D1500, SCI300, BCI and AUPP	22.7	0.2	0.2
KNeighborsRegressor	D1500, SCI300, BCI and AUPP	15.7	0.2	0.2
HuberRegressor	D1500, SCI300, BCI and AUPP	3.2	0.2	0.0

Table A4. Summary of Regression Analysis for FFWD E1 to Pave 3D 8K Surface Parameters

Model	Features	Accuracy (%)	MSE	R^2
LinearRegression	RD	6.9	3361027.8	0.1
GradientBoostingRegressor	RD	-6.7	3852809.2	-0.1
DecisionTreeRegressor	RD	-16.2	4195367.2	-0.2
RandomForestRegressor	RD	-9.4	3949513.3	-0.1
KNeighborsRegressor	RD	14.5	3086500.8	0.1
HuberRegressor	RD	4.9	3433876.3	0.0
LinearRegression	MPD	20.5	2376920.8	0.2
GradientBoostingRegressor	MPD	7.9	2755262.3	0.1
DecisionTreeRegressor	MPD	4.5	2855296.9	0.0
RandomForestRegressor	MPD	8.7	2731707.9	0.1
KNeighborsRegressor	MPD	10.7	2671732.4	0.1
HuberRegressor	MPD	19.0	2422029.3	0.2
LinearRegression	%CWP	-3.7	4044338.4	0.0
GradientBoostingRegressor	%CWP	38.1	2411803.3	0.4
DecisionTreeRegressor	%CWP	36.1	2491951.0	0.4
RandomForestRegressor	%CWP	40.6	2316457.2	0.4
KNeighborsRegressor	%CWP	41.3	2289104.5	0.4
HuberRegressor	%CWP	-11.2	4337394.0	-0.1
LinearRegression	%CNWP	5.8	2959374.9	0.1
GradientBoostingRegressor	%CNWP	-18.9	3735028.6	-0.2
DecisionTreeRegressor	%CNWP	-31.5	4129269.9	-0.3
RandomForestRegressor	%CNWP	-15.5	3625611.8	-0.2
KNeighborsRegressor	%CNWP	14.9	2673401.5	0.1
HuberRegressor	%CNWP	2.2	3072015.2	0.0
LinearRegression	RD and MPD	20.8	2860123.2	0.2
GradientBoostingRegressor	RD and MPD	22.1	2813313.1	0.2
DecisionTreeRegressor	RD and MPD	34.8	2355110.2	0.3
RandomForestRegressor	RD and MPD	41.2	2124008.8	0.4
KNeighborsRegressor	RD and MPD	40.7	2140338.6	0.4
HuberRegressor	RD and MPD	19.7	2898788.3	0.2
LinearRegression	RD and %CWP	10.8	3048954.9	0.1

Table A4. Summary of Regression Analysis for FFWD E1 to Pave 3D 8K Surface Parameters (cont.)

Model	Features	Accuracy (%)	MSE	R^2
GradientBoostingRegressor	RD and %CWP	58.9	1406018.0	0.6
DecisionTreeRegressor	RD and %CWP	37.9	2123096.5	0.4
RandomForestRegressor	RD and %CWP	54.1	1568488.2	0.5
KNeighborsRegressor	RD and %CWP	49.2	1736423.9	0.5
HuberRegressor	RD and %CWP	8.9	3114829.2	0.1
LinearRegression	RD and %CNWP	17.4	3092899.6	0.2
GradientBoostingRegressor	RD and %CNWP	28.6	2675620.6	0.3
DecisionTreeRegressor	RD and %CNWP	-29.4	4847579.3	-0.3
RandomForestRegressor	RD and %CNWP	45.3	2049376.8	0.5
KNeighborsRegressor	RD and %CNWP	51.8	1804647.9	0.5
HuberRegressor	RD and %CNWP	15.2	3177521.3	0.2
LinearRegression	MPD and %CWP	20.1	3117387.4	0.2
GradientBoostingRegressor	MPD and %CWP	46.1	2102083.2	0.5
DecisionTreeRegressor	MPD and %CWP	24.1	2957798.7	0.2
RandomForestRegressor	MPD and %CWP	54.7	1765462.1	0.5
KNeighborsRegressor	MPD and %CWP	42.6	2237970.3	0.4
HuberRegressor	MPD and %CWP	15.5	3293019.7	0.2
LinearRegression	MPD and %CNWP	24.5	2369932.4	0.2
GradientBoostingRegressor	MPD and %CNWP	36.0	2010504.5	0.4
DecisionTreeRegressor	MPD and %CNWP	4.9	2986201.1	0.0
RandomForestRegressor	MPD and %CNWP	33.8	2080276.0	0.3
KNeighborsRegressor	MPD and %CNWP	23.3	2408430.1	0.2
HuberRegressor	MPD and %CNWP	21.9	2452351.3	0.2
LinearRegression	%CWP and %CNWP	3.4	3225546.5	0.0
GradientBoostingRegressor	%CWP and %CNWP	54.3	1526204.2	0.5
DecisionTreeRegressor	%CWP and %CNWP	36.0	2138060.8	0.4
RandomForestRegressor	%CWP and %CNWP	53.8	1542259.5	0.5
KNeighborsRegressor	%CWP and %CNWP	36.1	2134756.0	0.4
HuberRegressor	%CWP and %CNWP	1.2	3299966.6	0.0
LinearRegression	RD, MPD and %CWP	19.2	2761987.6	0.2

Table A4. Summary of Regression Analysis for FFWD E1 to Pave 3D 8K Surface Parameters (cont.)

Model	Features	Accuracy (%)	MSE	R^2
GradientBoostingRegressor	RD, MPD and %CWP	53.6	1587673.2	0.5
DecisionTreeRegressor	RD, MPD and %CWP	44.2	1907180.1	0.4
RandomForestRegressor	RD, MPD and %CWP	55.8	1511847.5	0.6
KNeighborsRegressor	RD, MPD and %CWP	48.2	1771638.8	0.5
HuberRegressor	RD, MPD and %CWP	19.0	2769175.2	0.2
LinearRegression	RD, MPD and %CNWP	26.5	2754030.0	0.3
GradientBoostingRegressor	RD, MPD and %CNWP	66.8	1244004.7	0.7
DecisionTreeRegressor	RD, MPD and %CNWP	7.3	3473655.3	0.1
RandomForestRegressor	RD, MPD and %CNWP	58.8	1541758.4	0.6
KNeighborsRegressor	RD, MPD and %CNWP	61.4	1447715.7	0.6
HuberRegressor	RD, MPD and %CNWP	24.8	2818743.3	0.2
LinearRegression	RD, %CWP and %CNWP	32.1	1755093.3	0.3
GradientBoostingRegressor	RD, %CWP and %CNWP	52.5	1227359.0	0.5
DecisionTreeRegressor	RD, %CWP and %CNWP	15.8	2177503.8	0.2
RandomForestRegressor	RD, %CWP and %CNWP	50.0	1291869.8	0.5
KNeighborsRegressor	RD, %CWP and %CNWP	42.3	1491557.0	0.4
HuberRegressor	RD, %CWP and %CNWP	31.7	1767086.0	0.3
LinearRegression	MPD, %CWP and %CNWP	17.4	2760481.4	0.2
GradientBoostingRegressor	MPD, %CWP and %CNWP	57.8	1411266.6	0.6
DecisionTreeRegressor	MPD, %CWP and %CNWP	-1.8	3401835.1	0.0
RandomForestRegressor	MPD, %CWP and %CNWP	54.9	1508067.0	0.5
KNeighborsRegressor	MPD, %CWP and %CNWP	41.5	1952531.8	0.4
HuberRegressor	MPD, %CWP and %CNWP	17.1	2770361.0	0.2
LinearRegression	RD, MPD, %CWP and %CNWP	33.9	1708476.9	0.3
GradientBoostingRegressor	RD, MPD, %CWP and %CNWP	45.5	1408677.6	0.5
DecisionTreeRegressor	RD, MPD, %CWP and %CNWP	7.7	2387694.8	0.1
RandomForestRegressor	RD, MPD, %CWP and %CNWP	60.5	1022178.8	0.6
KNeighborsRegressor	RD, MPD, %CWP and %CNWP	61.5	996729.5	0.6
HuberRegressor	RD, MPD, %CWP and %CNWP	35.3	1673160.3	0.4

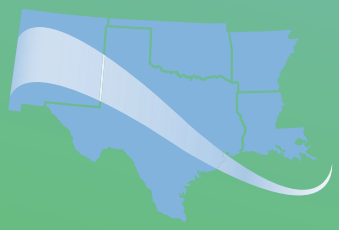

SOUTHERN PLAINS
TRANSPORTATION CENTER

The University of Oklahoma | OU Gallogly College of Engineering
202 W Boyd St, Room 213A, Norman, OK 73019 | (405) 325-4682 | Email: sptc@ou.edu